Chapter 7

Hydrophobicity — A Green Technique for Enhancing Corrosion Resistance of Alloys

Zaki Ahmad, Asad U. Khan, Robina Farooq, Naila Riaz Mastoi and Tahir Saif

Additional information is available at the end of the chapter

http://dx.doi.org/10.5772/60815

Abstract

The corrosion phenomenon is as old as the age of the planet. The cost of corrosion has risen alarmingly with industrial progress and it is estimated to be around 300 billion dollars or 3 to 4.5% of the GNP of developed nations. Thousands of alloys have been developed to control corrosion, which is a major consideration in the development of new ferrous and non-ferrous alloys. Several corrosion control techniques such as inhibitor treatment, coatings, cathodic protection, alloying additions, and designing for corrosion protection have been developed to combat corrosion. Despite their merits, techniques such as inhibition treatment and coatings are limited by their adverse effect on the environment because of their volatile organic components. Due to an increasingly alarming carbon footprint, there is a growing global concern to keep the environment clean. Hence, a great need exists to replace the current control methods by eco-friendly methods. The potential of the green technology of hydrophobicity has therefore been exploited to control corrosion by fabricating hydrophobic surfaces on alloys and these surfaces have shown highly promising results. This technology offers a novel method to control corrosion of metals, alloys, polymers and composites.

Keywords: Hydrophobicity, Wet contact angle, Sol-gel Technique, Potentiodynamic Polarization, Surface Roughness

1. Introduction

With the dramatic growth in technology witnessed during the last twenty years, new alloys have been developed to fulfill specific requirements for components in the aerospace, automo-

tive, shipping, transportation and metal industries. Researchers have focused their attention mostly on aluminum, copper, nickel, magnesium and ferrous alloys to enhance their mechanical strengths [1-16]. In recent years dramatic improvements have been made in enhancing mechanical, chemical and physical characteristics of ferrous and non-ferrous alloys by introducing nano-particles into the alloys. This is best exemplified by the nano-structured Fe. 20Cr alloy [17, 18] and the nano-crystalline surface of 304 stainless steel [19, 20]. The corrosion resistance depends on the formation of a passive and homogeneous film. Work on 304 stainless steel showed that the capability of passivation is enhanced, accompanied by enhanced corrosion resistance on a nano-structured surface [20].

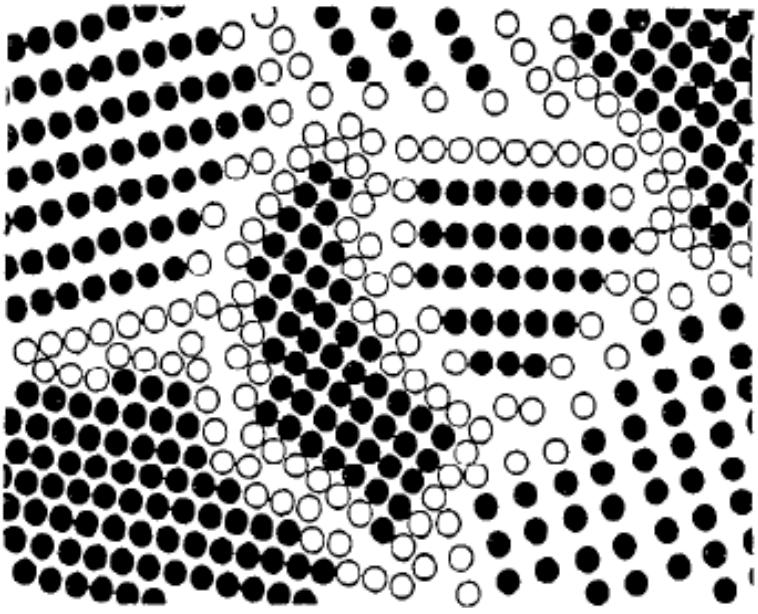

Figure 1. Schematic representation of the atomic structure of a two-dimensional nano-crystalline material distinguishing between the atoms associated with the individual grains (solid circles) and those constituting the grain boundary network (open circles) [24].

In both examples, the grain size cited ranged in the nano-scale regime. A study of 304 stainless steel prepared by equal channel angular processing with a grain size of 80-120 nm showed an improved tendency for passivation; studies on light alloys such as magnesium alloys showed the beneficial effect of nano-structured cerium oxide film. Potentiodynamic and electron impedance spectroscopy studies showed improved corrosion resistance of Mg alloy AZ31 [21]. The corrosion resistance of copper based alloys is attributed to the formation of cuprous oxide (CuO) and cupric oxide (Cu_2O) protective layers. They are excellent condenser tube materials for application in desalination plants [22]. The nickel development institute has done pioneering work on nickel and its alloys. Investigations have been conducted on nano-crystalline nickel alloy [23]. Enhanced overall current density is shown by nano-crystalline nickel and its

http://dx.doi.org/10.5772/60815

alloys because of high defects arising from the high surface fraction of grain boundaries and triple junctions. The high defect concentration provides increased number of potential sites, increased overall current density but reduced current density on individual sites which inhibits localized corrosion in nano-crystalline materials as shown in Figs. 1 and 2 [24, 25].
The grain growth is limited by triple junction (Fig 4) [25].

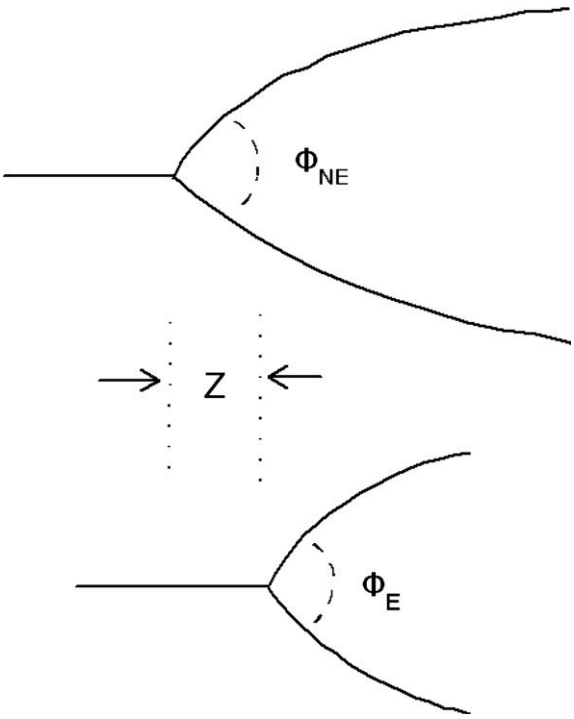

Figure 2. Schematic illustration of triple junction with (upper) non- equilibrium dihedral angle (Φ_{NE}) and (lower) equilibrium dihedral angle (Φ_E); migration of triple junction by distance z enables the retention of equilibrium dihedral angle [25].

Another factor is even distribution defect sites as compared to poly-crystalline materials. Nano-crystalline nickel shows uniform corrosion compared to severe localized corrosion in poly-crystalline nickel. The variation of anode/cathode current density in nano-crystalline materials depends upon the surface morphology and the surface modification as shown in Figs. 3 and 4 [26].

The decrease in corrosion resistance is attributed to the matrix/inter-crystalline (m/L) ratio and anode-cathode area ratios, which may decrease to 20 for grain size smaller than 100 nm. The uniformity of grain size may reduce penetration current density $i_a = i_c$. Improved corrosion resistance has been reported for nano-crystalline $Al_{90}Fe_5Gd_5$ and $Al_{87}Ni_7Y_{43}$ and $Cu_{90}Ni_{10}$ alloys [27, 28]. A nano-structured copper alloy showed less pitting corrosion attack than poly-

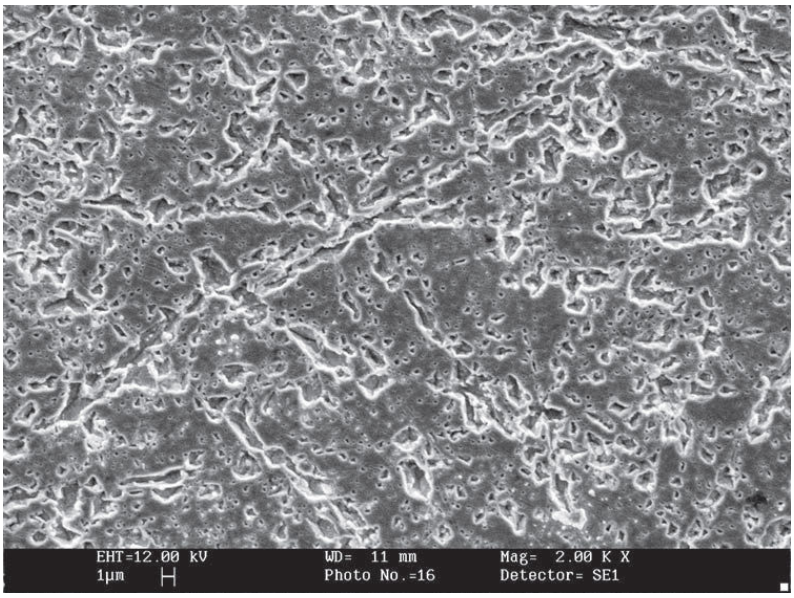

Figure 3. Surface morphology of nanocrystalline nickel [26].

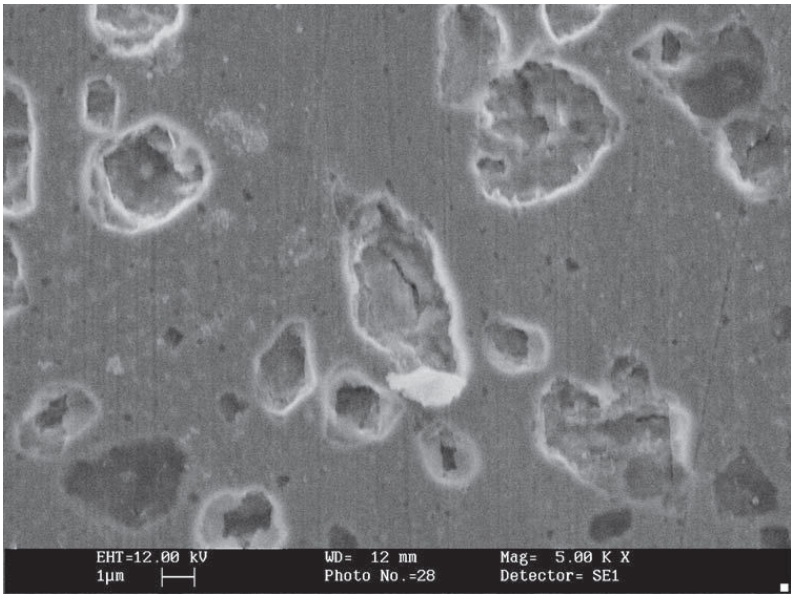

Figure 4. Surface modification to minimize corrosion [26].

http://dx.doi.org/10.5772/60815

crystalline copper electrode after polarization from 0.8 to 0.1V at 0.2 mv/S in a 3.5 wt% NaCl solution because of the formation of passive films of CuCl and Cu_2O [29, 30]. Studies on electrochemical behavior of nano-crystalline aluminum fabricated by plastic deformation showed enhanced passivation ability of nano-crystalline aluminum [31].

In a work, the addition of 0.3-0.4% scandium with 0.14% zirconium signally suppressed corrosion due to a passive layer created by the formation of nano-precipitates of Al_3Sc. A strong tendency of pinning of grain boundaries was observed. This shows how the grain size and nano-precipitates affect the passivation behavior of Al-Sc-Mg alloys [32, 33].

2. Cost of corrosion and bio-fouling

Although reliable figures and the most recent breakdown of corrosion losses have not been reported yet, from the recent past estimates the cost of corrosion is estimated to be around 85 billion dollars. In U.K, the cost is estimated to be 4-5% of GNP [34]. The corrosion free life of automobiles in the estimated cost of Saudi Arabia is only 6 months [35]. Corrosion costs are huge in land, sea and air transportation, oil and gas transmission pipelines and nano and micro-devices. In marine corrosion bio-fouling is encountered which affects the speed of ships and causes excessive consumption of fuels. Marine bio-fouling has manifold effects on the corrosion and life cycle of marine vehicles and plants using sea-water such as dual system desalination plants. The condenser tubes become the target of corrosion bio-fouling. Bio-fouling affects marine vehicles such as ships and boats by the adhesion of layers of micro-organisms and deposition of bio-films. Their attachment to the substrate also leads to the formation of differential aeration cells and onset of localized corrosion. The active organisms which attack are generally bacteria, diatoms, algae and invertebrates causing increased hydrodynamic drag resulting in increased fuel consumption [36].

Both chemical and physical methods have been used to control bio-fouling. The circulation of sponge rubber ball with cooling water has been employed conventionally. The use of a suitable polymers has been quite successful. Biocides have been used to kill micro-organisms. Glute-aldehyde as well as proprietary mixtures of complex organic compounds has been extensively used. Despite all research, the development of a bio-film repellent surface appears to be a new remedy which is being resolved by super-hydrophobic surface. The damaging effects are not only limited to corrosion and bio-fouling, but they also affect the environment. The international maritime organization estimates that fuel air emission could increase between 38 and 72% by the year 2020. Anti-fouling coatings have been developed from natural resources; however their behavior is not conclusively known. Low surface energy nano-SiO_2 coatings have the capability to reduce the adhesion strength of micro-organisms. The micro, nano-layer structures on the coating films could be obtained when an appropriate mass ratio of resin, nano-SiO_2 and other pigments are approached. Sea-water tests have shown that lower surface energy and the elastic modulus of coatings are less in adherence of the bio-films [37].

The technology of super-hydrophobic surfaces has come to the rescue of bio-fouling. Super-hydrophobic surfaces are defined as surfaces with wet contact angle greater than 150^o. These

surfaces are water repellent and due to their hierarchical nature of surface and deposition of low energy compounds, they repel water. This phenomenon will be fully described under "Super-Hydrophobicity theory" to understand super-hydrophobic coatings which lower the surface energy of a substrate. In a work reported, a super-hydrophobic surface attached significantly less micro-organisms after nine days on silicon coated enamel, fluorinated ethylene propylene (FEP) abutments and modified silicon rubber voice prosthesis with fluoroalkyl-silanes showing a significant reduction in bio-film formation [38-40]. A few strategies have been adopted to mitigate bio-fouling. The hyper-branched fluoropolymers (HBFP) and polyethylene glycol (PEG) film showed a strong resistance to proteins, serum, albumen, lectin, and lipopoly-saccharides [41].

In another study amphiphilic block polymers, co-polymers based on polystyrene (PS) and polyacrylate (PA) were designed. The PS block acted as a binder and PA block exposed the amphiphilic side chain to the exterior. These materials showed a good resistance against ulva and cells of diatoms [42]. The application of hydrophobic surface exposed to marine environment has shown a dramatic change since 1926, when Navy used plastic paints to prevent bio-fouling. The use of anti-adhesive water repellent surfaces is a departure from polymer technology practiced in the past.

3. Corrosion protection methods

Conventional corrosion protection methods include alloying, coating, designing for corrosion protection, cathodic protection and surface modification, inhibition and selection of materials for a particular environment. There is a vast amount of literature available on these conventional methods in books and journals on corrosion such as "NACE Corrosion and Materials Protection" published by NACE, Houston Texas, U.S.A. and other corrosion journals [43-48]. All the conventional methods have their merits and they are highly productive. It is very well known that water, moisture, humidity, acid and basic electrolytes and marine environment induce corrosion in different forms. It was not until the lotus effect was discovered by Barthlott and Neinhuis [49] on lotus leaves that research was focused on hydrophobicity and hydrophilicity as a tool to mitigate corrosion.

Super-hydrophobicity is now the focus of attention because of its promising application potentials on increasing life cycle of metal and alloys, cleaning of environment, reduction of drag in ocean going vessels, anti-icing of aircrafts, properties minimizing reduction of drag speed of ships, corrosion of materials, control of bio-fouling, enhancement of heat transfer on condenser surface and conservation and conversion of energy [50-52].

4. Hydrophobicity

Hydrophobicity or water repellency is an inherent property bestowed by nature on some plants, the most significant being the lotus. While the lotus plant stays in dirt, it remains clean

http://dx.doi.org/10.5772/60815

as its leaves repel water which is deposited in the form of droplets and flows away. A similar phenomenon is attached to several other plants and insects such as the desert beetle (steno cava). Thus a natural phenomenon has been mimicked and hydrophobic engineered surfaces have been fabricated on metallic and nonmetallic substrates. Hydrophobicity is defined by wet contact angle formed between the droplet and the substrate. If this angle is greater than 90°, the surface is called hydrophobic and if greater or equal to 150°, the surface is called super-hydrophobic. Super-hydrophobic surfaces also show low contact angle hysteresis. As demonstrated by lotus leaves, there are basically two requirements for a surface to be hydrophobic;

a. The surface must have a roughness in the range of 4-6 μm.

b. The surface energy must be very low or made lower by deposition of low energy compounds like polydimethyl siloxanes (PDMS).

A hierarchical surface is the key to hydrophobicity. A hierarchical surface is characterized by a structure comprising of microhills and valleys with epicuticular crystals of wax as found in the lotus flower and nano-hairs found in the gecko. The grain size is also an important feature as the grains need to be in the nano-regime, less than 100 nm. The hills are also called asperities. The surface area of asperities being very small, water drops cannot be attached and consequently they roll down. Increasing the roughness of a surface increases its wettability. When the wet contact angle between substrate and liquid becomes greater than 90°, the surface becomes hydrophobic. When a liquid drop is deposited on a flat surface as shown in Fig. 5 [53], the wettability is determined by the chemical composition of the surface; the intrinsic water contact angle $\varnothing_{flat}$, can be co-related to interfacial free energies, that is free energies at the solid air (γ_{SV}), solid liquid (γ_{SL}) and liquid air (γ_{LV}). By Young equation [54],

$$Cos\ \varnothing_{flat} = \frac{\gamma_{SV} - \gamma_{SL}}{\gamma_{LV}} \tag{1}$$

the expression γ_{SL} can b estimated by

$$\gamma_{SL} = \gamma_{SV} + \gamma_{LV} - 2\sqrt{\gamma_{SV} \cdot \gamma_{LV}} \tag{2}$$

Equations 1 and 2 indicate that hydrophobicity increases with decreasing the surface energy of the solid-air (γ_{SV}) interface. The lowest surface energy is possessed by trifluoromethyl (CF_3) group terminated surface (~ 6 mN/m) with an $\varnothing_{flat\ of}$ 120° [55].

It may be noted that low surface energy as the major factor and roughness only enhances it. The contact angle on an ideally rough surface is shown in Fig. 6 [53]. Wetting on rough surface was discovered by Wenzel [56] and later followed by Cassie and Bexter [57]. Wenzel suggested that if the droplet filled the roughness counters, it should enhance hydrophobicity with a linear relationship between contact angle and roughness given by;

$$Cos\ \varnothing^{W}_{rough} = \gamma cos\varnothing_{flat} \tag{3}$$

where $\varnothing$ = static contact angle

and $\varnothing^{W}$ = apparent contact angle enhanced by roughness

$$\text{Roughness}\gamma = \frac{True\ surface\ area}{Horizontally\ projected\ surface\ area} \tag{4}$$

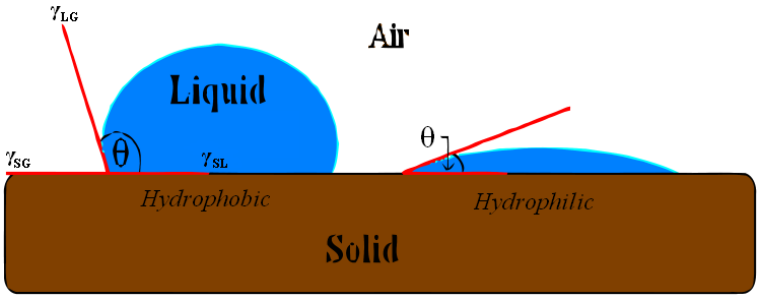

Figure 5. Contact angle made by droplet on hydrophobic (Left) and hydrophilic surface (Right) [53].

As surface roughness is greater than 1, the equation predicts that, $\varnothing_{flat} > 90^{o} >$, $\varnothing_{rough} > \varnothing_{flat}$ and if $\varnothing_{flat} < 90^{o}$, $\varnothing_{rough} < \varnothing_{flat}$.

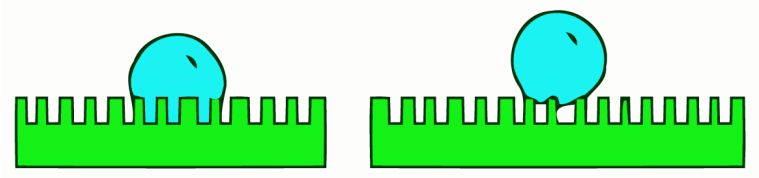

Figure 6. Theory of droplet formation on a rough surface. Fully wetting the surface contours (Left) and suspension on a solid/air composite (Right). These are the two basic models in SH theory [53].

Hence in the Wenzel state, increasing surface roughness will make surface more hydrophobic and intrinsically hydrophilic surface more hydrophilic. If, however, the surface roughness is increased, it becomes difficult for water to be in complete contact with the substrate. The air is likely to be trapped between water and the surface texture, which is called a composite surface. The water comes in contact with a composite surface of solid and air and forms droplets. In this case the contact angle is described by the Cassie Bexter equation [57]. The apparent contact angle described by Cassie Bexter is

http://dx.doi.org/10.5772/60815

$$\text{Cos } Ø_{rough} = Ø.\text{Cos } Ø_{flat} + ØV.\text{Cos } Ø_{LV} = Ø_S.\text{Cos } Ø_{flat} - \left(1 - Ø_S\right) \quad (5)$$

$Ø_S$ and $Ø_V$ are the fractions of solid and air contacting with water ($Ø_S + Ø_V = 1$). Since the contact angle of water on air ($Ø_{LV}$) is 180°, ($\text{Cos } Ø_{LV} = -1$), that is, air entrapped would increase the surface hydrophobicity. As shown by Eq.(5), monotonic decrease of $Ø_S$ would increase $Ø_{rough}$ with an eventual increase in hydrophobicity. Figure 7 [58] shows the relationship between $Ø_{rough}$ and $\text{Cos } Ø_{flat}$. The two states are illustrated in Figs. 8 [58] and 9 [58].

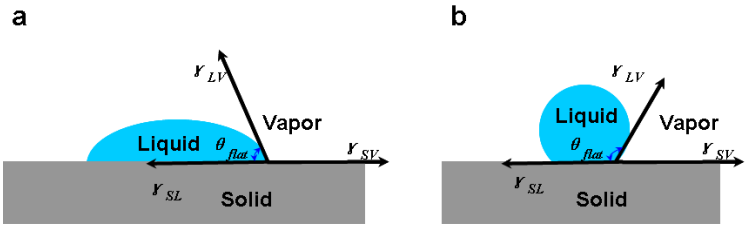

Figure 7. Contact angle of a liquid on an ideally flat surface (Young's model). For water, if θ_{flat} <90°, it is an intrinsically hydrophilic surface (a); if θ_{flat} >90°, it is an intrinsically hydrophobic surface (b) [58].

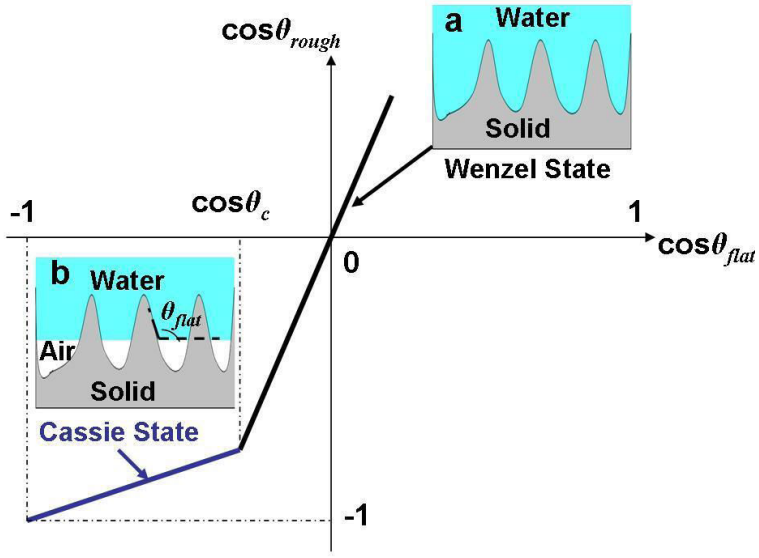

Figure 8. Relationship of $\cos\theta_{rough}$ with $\cos\theta_{flat}$. The black solid and blue solid lines correspond to the Wenzel state and the Cassie state, respectively [58].

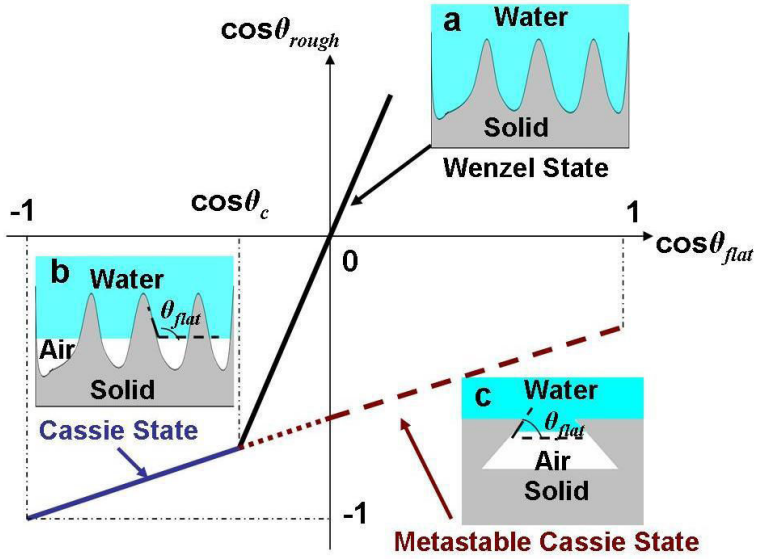

Figure 9. Relationship of *rough* cosθ with *flat* cosθ. The dotted and dashed lines correspond to the metastable Cassie state when cos> 90° *flat* θ and the metastable Cassie state when cos< 90° *flat* θ, respectively [58].

The research on super-hydrophobic surfaces faces several challenges such as the durability of a hydrophobic surface and stability. Another problem faced is the contamination of their surfaces by oil as such surfaces are not oil repellent. A few oil repellent surfaces have been reported; however, oil contact angles have been reported with oils of high free energy (γ_{LV}> 30 mN/m) such as polyols esters, arcnes and their mixture [55, 59, 60].

In recent findings on the role of super-hydrophobic surfaces in condenser tube, it has been shown that the heat transfer coefficient can be enhanced by water droplets falling on a condenser tube with a super-hydrophobic surface; however, the major problem is the with-standing of high temperature and stability of the surface [61]. Attempts have been made to produce high temperature surfaces using macro-porous silicon and to achieve a wet contact angle of 155º [62]. A lot of work remains to be done on corrosion wear, fatigue, and bio-fouling resistance of super-hydrophobic surfaces. Research in progress shows highly promising application potential of hydrophobic surfaces in the near future.

5. Methods of fabrication of hydrophobic and super-hydrophobic surfaces

Several techniques have been employed to generate hydrophobic surfaces. Modified paint technology has been used to produce super-hydrophobic surface. The paint (binder + pigment + particles + solvent) are the major constituents of paint. By keeping particles loading high and

http://dx.doi.org/10.5772/60815

binder content low, the binder evaporates and the particle adheres with the binder which roughens the surface. Major techniques employed to create hydrophobic surfaces are described below.

5.1. Layer by layer deposition

The fabrication of multi-composite films by layer by layer procedure means literally the nanoscopic assembly of hundreds of different materials in a single device. The film displays close to identical properties after deposition of first few layers. By utilizing the attraction between electrostatically utilized charged particles, one can form a multi-layer structure by dipping a substrate in a positive and negative charged polyelectrolyte. For instance, a microporous substrate can be generated by mixing polymer, polyalkylamine hydrochloride (PAH) and polyacrylic acid (PAP) and coating it with silica nanoparticles. This technique has several advantages, such as longer adsorption time which gives good adhesion, the desired thickness, and uniformity of surface. The cross-contaminate of deposition solution is also avoided as it may lead to depletion of the concentration of adsorbing molecules. It offers a very large processing window; hence, it is important to keep the processing conditions constant.

LBL technology allows us to design functional surfaces and surface based nano-devices in a build to order fashion. It exceeds simple self organization under equilibrium condition by its capability to arrange different materials at will in the presence of a nano-scale. In this procedure, self assembled technique enables deposition of multi-layer films on non-flat surfaces. By employing LBL technique, a super-hydrophobic surface was prepared by depositing silica nanoparticles on the surface of a 10 bilayer poly acrylic acid (PAP) coated ZrO nanoparticles polyallylamine hydrochloride (PAH) film followed by simple fluorination [63, 64]. LBL assemble allows deposition of multi-layers on non-flat surface. It has been shown that multilayer films of poly diallyl dimethylammonium chloride (PDDA)/sodium silicate films can be deposited by LBL techniques. It is a simple and expensive way to create hydrophobic surface obtained by coating positive and negative polyanions in a sequence, the last layer being hydrophobic.

5.2. Electrochemical methods

They are widely used to form hydrophobic surfaces on rough structures. For example, Gold clusters have been electrochemically deposited on the matrix of polyelectrolyte multiple layers [65, 66]. Rough surfaces required for deposition of hydrophobic films have been fabricated by electro-deposition. Polymers can be deposited electrochemically with ease as they are inherently hydrophobic. Complete object can be coated by electrodeposition. Super-hydrophobic surfaces of silver, zinc oxides, and copper have been fabricated by electrochemical methods [67-69]. To make an aluminum surface hydrophobic, it is first anodized in an acid at specific voltage to create pores and the oxide layers, before applying a hydrophobic coating such as perfluoroallylsilane. A hydrophobic film of myristic acid can be deposited on copper by electrochemical technique.

5.3. Plasma and laser treatment

Plasma deposition can be used to produce hydrophobic surfaces directly as exemplified by deposition of polymers. Treatment by polymer leads to shrinkage and generates roughness on the surface. Some single step methods have been used to produce hydrodynamic surfaces as shown by treatment of silicone in CF_4. Laser treatment is more effective than plasma deposition because the vaporized material is re-deposited in cluster and the treated surface. The plasma technique provides a convenient tool to produce surface with special optical properties. The success of its method is shown by the preparation of fluorinated super-hydrophobic surface [70, 71].

5.4. Chemical and physical vapor deposition

Hydrophobic surfaces have been prepared by microwave plasma enhanced chemical vapor deposition (CVD) using organic silicon compounds and inert atmosphere using argon gas. By introducing CO_2 as an additive gas, ultra-pure water repellent films have been obtained. Super-hydrophobic surfaces using perfectly aligned carbon nano-tubes forest have been produced. Physical vapor deposition technique has also been used to produce super-hydrophobic surfaces of n-hexatriacontane [72-74].

5.5. Electro spinning

It is the use of electrostatic force to draw a thin fiber with a viscous polymer liquid on a substrate. For this purpose, polymer solutions, liquid crystals, suspensions of solid particles, and emulsions are electro-spun in an electric field at 1 KV. After the jet flows from the droplet in a straight line, it bends into a complex path which brings about changes in shape during which the electrical forces thin it. The solvent evaporates and bare fringent nanofibers are left.

Spinning can produce fibers down to micrometer and nanometer sizes from a wide range of materials including carbon fibers and carbon nano-tubes. Super-hydrophobicity is obtained without any modification. Cotton fibers have been coated with carbon nano-fibers and have shown good resistance against hot water [75, 76].

5.6. Sol-gel process

The sol-gel process involves the evolution of inorganic network through the formation of a colloidal suspension (sol) and gelation of the sol to form a continuous network. The pre-cursors of these colloids consist of a metal or metalloid element surrounded by reactive ligands. The most widely used aloxides and alloxysilanes, for example, tetramethoxysilane, metal oxo-polymer are obtained by polymerization reactions through hydrolysis and condensation of metal alkoxides $M(OR)_2$, M=Si, Ti, Zr, Al, An, Ce.

Super-hydrophobic surfaces have been created by combination of silicon particles, polymer binder, and hydrophobizing agents. Silica is used in the form of silica sols. The silica sol is used in sol-gel reactions where a combination of hydrolysis and condensation reactions of oxide structures takes place. The reactions are shown below:

http://dx.doi.org/10.5772/60815

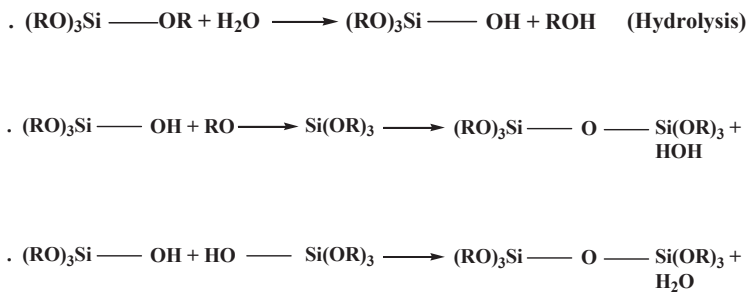

Reaction 2 and 3 are condensation reactions. The silica properties can be made hydrophobic by treating with different silane. Surface modifications occur by a reaction between the silanol groups of the silica surface and the silanes, as shown in Fig. 10. Compounds like fluoroalkyl-silanes are excellent hydrophobic agents due to their low surface energy. Several different silanes made by Dow Corning have been used as hydrophobic agents [77-80]. The sol-gel technique provides a simple and cost effective method for the preparation of super-hydrophobic surfaces. Most of TiO_2 coatings with silanes have been prepared by sol-gel technique. The SiO_2- TiO_2 coatings in photocatalytic reactors have largely used this technique.

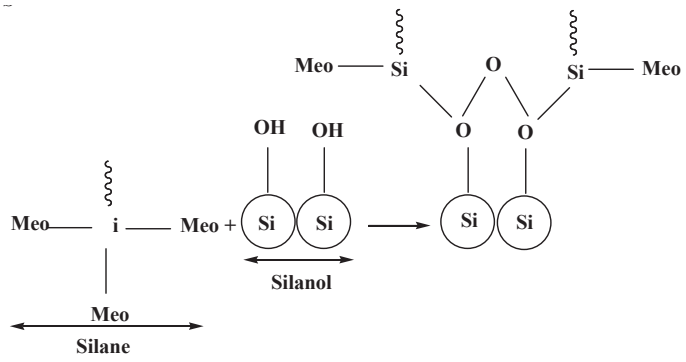

Figure 10. Surface modification of the substrate by silanol.

Water repellent, UV protective and anti-microbial coatings have been fabricated on textile fiber. Hydrophobic coatings on glass have been produced by sol-gel techniques using fluorinated compounds. Fluorinated silica nanoparticles have been produced by sol-gel process for production of super-hydrophobic films on glass, FAS 13 (fluoroalkyl-silane) was used to create hydrophobicity [81].

5.7. Self-Assembled Mono-layers (SAMS)

These are molecular assemblies formed by exposing the substrate in a solution of active surfactant in an organic solvent. It is best illustrated by alkanethiols which bears a hydrophobic

alkyl chain and a thiol group which acts as an anchor. The SAMS of alkanethiol were applied on Golu surface [82]. Low surface energy coatings were developed on glass slides, silicon wafers, silicon nanoparticles, and zeolites by using organic silanes. A contact angle of 154^{o} was obtained by modification of a SAM of octyldimethoxy silane. Fatty acids have also been employed for fabrication of super-hydrophobic surface such as copper [83-85].

5.8. Lithographic techniques

The basic idea is to expose a photo-resistant polymer to radiation through a photo-mask and remove the exposed or the unexposed paints depending on the nature of polymer. The patterned polymers can be directly used or can be used as a mask for deposition and etching. Nano-patterned lithography can also be used. One promising method is to directly use the dual scale surface roughness of surfaces found in nature such as lotus leaves or wings of cicada as stamps. The surface is pressed in PMMA at an elevated temperature. This is followed by transferring the pattern to a silica substrate.

Lithography is a well known technique for creating a rough surface. Patterns of mask were transferred onto silicon wafers followed by using hydrophobizing by silanes. The spin coating of mono-dispersed polystyrene beads for lithography is used to obtain large and periodic nano-sphere arrays. The nano-spheres are coated with gold film and modified with octadeca-nethiol. The hydrophobic surface can be tuned from 132^{o} to 170^{o} [86-88].

5.9. Phase separation

Due to coating or change of pressure, phase separating begins and a bi-continuous network is formed; if one of the phases becomes solid, the remaining liquid can be removed, forming a bi-continuous, three-dimensional network. In case the desired wet contact angle is not obtained, an additional super-hydrophobic coating can be applied.

5.10. Chemical etching

Besides lithography, chemical etching is another useful technique which has been successfully employed on steel and glasses. Rough surfaces on stainless steel were created by using hydrofluoric acid. After the deposition of fluorocarbon film, the etched samples of 304 and 316 stainless steel displayed a wet contact angle of 159^{o} and 146.6^{o} respectively [89]. Composition of etchant and time of exposure of substrate in the etchant have a significant bearing on the wet contact angle.

6. Super-hydrophobic surfaces and corrosion behavior

Corrosion is a serious problem in engineering systems such as automobiles, aircrafts, oil and gas transmission pipelines and ocean vehicles, reinforced concrete, and in micro- and nano-mechanical devices. Whereas traditional methods such as alloying, inhibition addition, cathodic protection, coatings, and designing for corrosion protection have been very beneficial,

http://dx.doi.org/10.5772/60815

the development of hydrophobic films have opened a novel route for corrosion mitigation. A brief review of the application of hydrophobicity to control corrosion is presented below. The application of hydrophobicity on steels, aluminum, magnesium, copper and their alloys is the focus of review.

6.1. Effect of hydrophobic surface on the corrosion resistance of aluminum alloys

Aluminum alloys 6061, 6013, 5052, 7075 and 2024 are well known for their excellent corrosion behavior in marine environments; however, the effect of hydrophobicity on their corrosion behavior is yet to be highlighted. Sulfuric acid, oxalic acid and phosphoric acid have been mainly used as electrolytes in anodizing to increase the wet contact angle.

Anodizing of aluminum alloys is also performed in chromic acid electrolyte followed by sealing in potassium dichromate to improve the corrosion resistance. Despite the use of several sealing products such as molybdate, cerium (IV), boric acid (V), Chromium (VI)N, and tartaric acid, these sealing agents need further improvement. A new procedure developed involves the use of carboxylic acids for post-treatment after anodizing. In an experiment conducted on Al 2024, anodizing experiments were carried out in 40 g/L in presence of 80 g/L of tartaric acid at a voltage of 14V for 20 min. Four different types of carboxylic acids, hexanoic acid, decanoic acid, myristic acid and stearic acid have been used. The contact angle increased from 10° to 110° by treatment with decanoic acid. This shows that carboxylic acid reacts with aluminum hydroxide to form an organic film which shows strong hydrophobic properties. Results of impedance spectra and salt spray tests showed decrease of corrosion due to the formation of hydrophobic films. Plots after and before and after post-treatment are shown in Fig. 11 [90]. Using myristic acid, a super-hydrophobic surface was created on aluminum alloy by anodizing and hydrophobization by myristic acid. The results showed that the super-hydrophobic coating with a contact angle greater than 160° decreased the corrosion rate tenfold compared to untreated aluminum. The contact angles measured on anode layer after treatment are shown in Fig. 12 [90]. The super-hydrophobic surface mainly affected the anodic reaction. The corrosion current (Icorr) was reduced by their orders of magnitude and the corrosion potential (Ecorr) shifted positively by 0.2V, indicating a significant reduction in corrosion rate [91, 92].

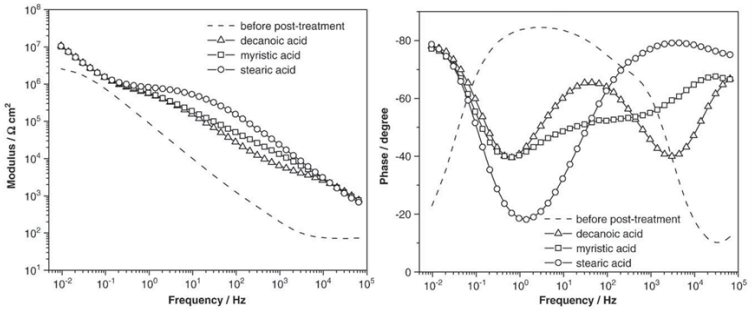

Figure 11. Bode plots of unsealed anodic layers obtained before or after post-treatment for 30 min 75 °C in pure molten acids (diagrams plotted after 2 h of immersion in 0.5 M Na_2SO_4) [90].

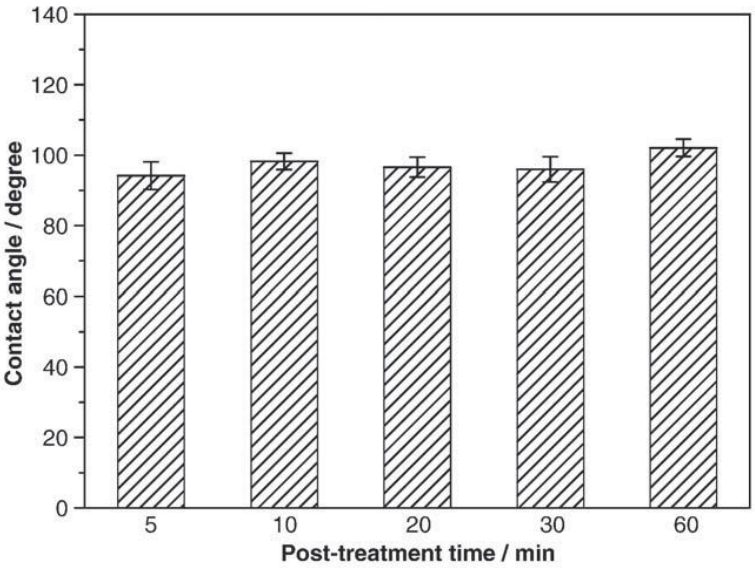

Figure 12. Contact angles measured on the surface of sealed anodic layers after post-treatment for 5-60 min at 75 °C in pure molten stearic acid [90].

It has been demonstrated that the super-hydrophobic surfaces prevent adherence of bio-fouling organisms. Work on scandium (Sc) doped Al-Mg alloys showed that addition of 0.3-0.4% Sc with 0.14% Zirconium (Zr) enhances their corrosion resistance due to the formation of Al_3Sc nanoparticles. These ultra-fine precipitates allow the formation of a highly uniform film of ScO_3 with boehmite. Different types of precipitates are shown in Fig. 13 [32].

Some advanced work showed that reaction of the substrate by myristic acid and perfluorosilane enhance the corrosion resistance three-fold as compared to untreated samples [32, 93].

In a work, water based silica films were applied on aluminum alloy 6082 and AZ31. The water based sol was prepared from 3-glycidoxypropyltrimethoxysilane (GPTM), triethylorthosilane (TEOS), water as a solvent and acid as a catalyst. The sol with TEOS showed that it acts as a barrier to water penetration. The hydrophobicity was enhanced by addition of GPTM. The cyclic voltammetry (CV) measurements showed pitting corrosion for uncoated aluminum and magnesium alloy in chloride solution, whereas no corrosion was observed in the substrate coated with silica film. The corrosion current density of coated sample was 3.96E-3mA/cm^2 for aluminum. Sample 6082-T6 was coated with silica film. The silica coated substrate enhanced the protection efficiency to 96.68%. This is attributed to the bonding of the silica film to substrate through covalent bonding thus ensuring its adhesion. The SiO_2 particles may react with OH^- ions which are generated from the cathode. The passive silica layer minimized the corrosion of aluminum alloy. This also applies to magnesium alloy AZ31. The corrosion current density of uncoated aluminum sample was 3.96 μA/cm^2 and 0.052 μA/cm^2 for sample coated with silica film. The protection efficiency is defined by:

http://dx.doi.org/10.5772/60815

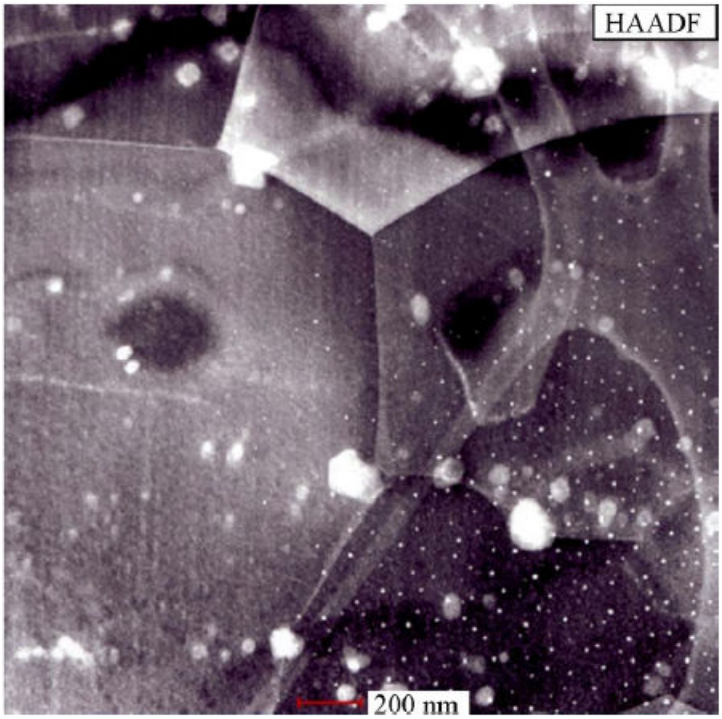

Figure 13. Different types of precipitates are clearly shown in HAADF STEM image. Al3Sc precipitates on the grain boundaries and homogeneous distributes of nano-precipitates are observed [32].

$$\text{P.E C\%} = \frac{\mathbf{I}_{\mathbf{corr\,(uncoated)}} - \mathbf{I}_{\mathbf{corr\,(coated)}}}{\mathbf{I}_{\mathbf{corr\,(uncoated)}}} \times 100$$

The polarization curves are shown in Dig.14 [94].

Studies in super-hydrophobic treatment and corrosion protection for aluminum in sea-water were undertaken to evaluate its effectiveness [94]. Anodization was carried out at a current density of 0.32A/cm^2 in a 15 wt% of sulfuric acid at 27V, the time duration being 7 min. The sheets were modified by melting in myristic acid for 30 min at 70^{o}C and washed in ethanol at 70^{o}C and de-ionized water followed by drying in oven. Potentiodynamic electrochemical studies were conducted in the potential range of 600-60+ mV at a scan rate of 2 mV/s. Electrochemical impedance was performed by IMC electrochemical work station. Nano-spheres of diameter 50-60 nm was observed. The roughness was about 2 μm after hydrophobization with myristic acid, and a leaf like structure was obtained, as shown in Fig. 15 [94]. The potentiodynamic and bode plots of specimen under treated and untreated conditions are shown in Fig. 16 [94].

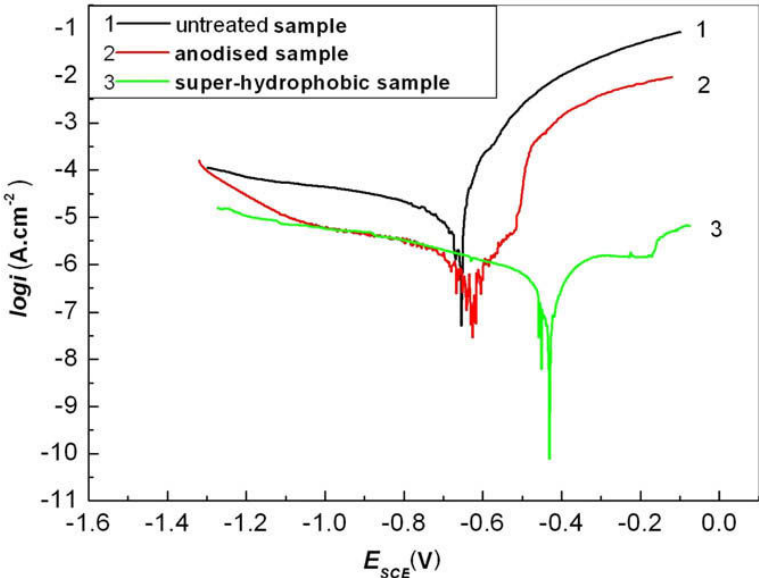

Figure 14. Potentiodynamic polarization curves of untreated, anodized, and super-hydrophobic samples for 24 h in sterile seawater at 2 mV s^{-1}[94].

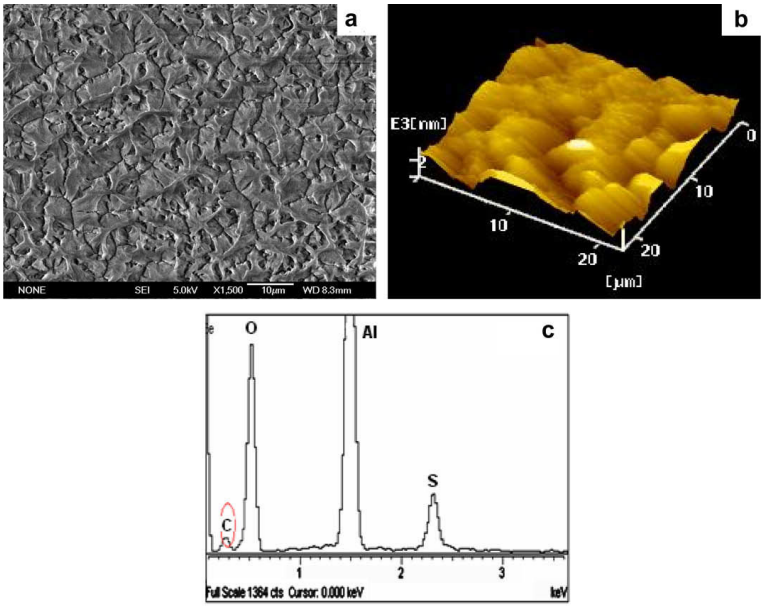

Figure 15. (a) SEM, (b) AFM, and (c) EDS of the super-hydrophobic aluminum surface [94].

http://dx.doi.org/10.5772/60815

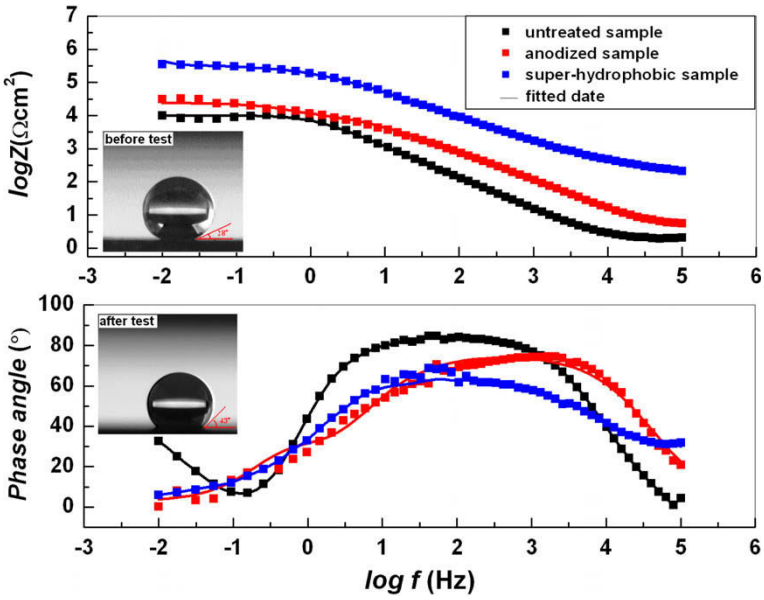

Figure 16. Bode plots of untreated, anodized, and super-hydrophobic samples after immersion in sterile seawater (32‰ NaCl, pH 8.02) for 24 h with the contact angle images of the super-hydrophobic surface before and after EIS test [94].

The porous anodic aluminum oxide was subjected to corrosion by penetration of chloride ions, where excellent corrosion resistance was shown by the surface modified with myristic acid. The basic requirement for corrosion prevention is to minimize the wetted area. It depends on whether the film is stabilized within the roughness grooves. It may be noted that air is trapped in the grooves which makes it a composite surface. The air entrapment would be metastable for the condition.

$$90 \leq \leq \cos \frac{f_1 - 1}{\gamma - f_1}$$

where f_1= ratio of area of liquid beneath the drop in contact with solid

γ = roughness ratio of the surface

$\varnothing$ = contact angle

If the $\varnothing$ is > 90°, the air would be entrapped. As a contact angle of 138° was observed, it showed that the film was stabilized within the grooves, which minimized the migration of chloride species to the surface and hence the substrate was protected. The corrosion behavior of magnesium alloys coated with fluoroalkylsilane molecule in corrosive NaCl has been investigated [21].

In the investigation, magnesium alloy AZ31 (29.8% Al, 0.88% Zn, 0.38% Mn, 0.0135% Cu, 0.002% Fe, and balance Mg) with a thickness of 1.5 mm was used. After cleaning, the alloy was immersed in 50 ml of distilled water containing 1.086 g of cerium nitrate hydrate ($Ce(No_3)_3.6H_2$). After final washing, the samples were immersed in 40 m toluene solution containing 400 μL of fluoroalkylsilane ($CF_3(CF_2)_7CH_3CH_2Si.(CH_3)_3$) and 40 μL of tetramethyl-siloxy titanium (TEST) for 30 min to deposit a hydrophobic film. No change in surface morphology revealed a porous structure after 1440 min; the nano-structured cerium oxide layer is comprised of a porous layer in contact with the substrate and intermediate compact layer and fibrous top layer. The averaged wet contact angles ranged between 136±2° to 152° after 360 min and indicated no significant change after immersion. However after 1440 min, significant change in wet contact angles occured which indicated enhancement of corrosion. The surface morphologies showed no significant change after immersion for 180-360 min. The formation of granular products increased with increased exposure time. The corrosion product was identified as $Mg(OH)_2$.

Potentiodynamic curves of untreated alloy in 5% of NaCl for 30 min and super-hydrophobic surface formed after 30, 60, 18 and 144 min was analyzed. The untreated alloy showed higher current densities compared to the treated alloy with hydrophobic surface. The EIS measurement also indicated as improvement in corrosion resistance. The studies present conflicting results for exposure periods exceeding 360 min. The substitution of self-assembled mono-layers as an alternate for coatings on aluminum has been investigated in recent years [96, 97]. It is to be re-called that the molecules which constitute SAM have three major characteristics:

a. The functional group adheres to the substitute

b. The aliphatic chain acts in the self-organization process

c. A functional group is exposed on top of the layer

SAMS condensation over aluminum surface has shown that methoxy-silane monolayers, for example octadecylmethoxy silane (ODMS) and propyltrimethoxy silane (PTMS) protect aluminum base materials as these molecules form very compact coatings on oxalic surfaces. The SAM coated aluminum alloy 7075 surface showed that the SAM layers coated substrate showed a potential shift in the positive direction. The ODMS mono-layer showed superior properties over PTMS. The siloxane SAMs appear to hold a promising potential not only for Al 7075 but for most aluminum alloys used for marine applications. The major problem with Al 2024 is their enrichment in copper content which acts as a cathodic and initiates the possibility of a galvanic attack. SAMs were formed on 2024-T3, using decyltriethoxy silane (DTES) and n-octadecyltriethoxy silane (ODTES). The SAMs were created by converting ethoxysilanes ($R_3SiOCH_2CH_3$) to silanol (R_3SiOH). The ethoxy-silanes were hydrolyzed to silanols in solution of 0.02 silane, 0.006M HCl, and 0.28M H_2O in ethanol. The solution was hydrolyzed and diluted by a factor of 10. The alloy was immersed in the solution. This was followed by a condensation reaction resulting in the formation of M-O-Si bond. The curing temperature was 50°C. Water contact angles of 113° and 117° were obtained with decatriethoxy silane and n-octadecyltriethoxy silane, respectively [98]. As shown by electrochemical studies, the corrosion potential values (Ecorr) are shifted in the positive direction compared to the bare

http://dx.doi.org/10.5772/60815

surface. The suppression of corrosion was clearly evident due to suppression of anodic dissolution. The results on anodic dissolution would depend on whether the SAM is attached to the oxide surface or directly to the substrate as alkanethiol SAMs on iron and copper showed no significant change in anodic currents [99, 100].

These methods yet remain to be applied on a large scale to fully explore their benefits. The effect of SAMs on the corrosion resistance of alloys like 6061, 6013 and 5052 needs more attention of researchers because of their increasing demand for industrial application in automotive, transport, desalination plants, and marine vessels. More work is required to understand the mechanism of corrosion of the hydrophobic surface for long term and short term duration.

6.1.1. Role of nano-pores on the hydrophobicity of aluminum alloys

Nano-pores play a crucial role in controlling hydrophobicity and corrosion resistance of aluminum alloys. Hence, the role of nano-pores on anodized aluminum needs to be better understood. More research needs to be focused on the role of nano-pores. The anodized aluminum is used as a template for the creation of ordered nano-structures. This requires ordering of the nano-pore as shown in Fig. 17.

The formation of nano-pores depends on the electrolyte used and the voltage applied. Anodizing potential has a significant effect on pore formation. An increase in temperature increased pore diameter. Pore diameter may be increased in an acid solution, such as phosphoric acid. A cross section of porous aluminum is shown in Fig. 18 [101]. The pores are hexagonal in shape. Important parameters of pores are pore diameter, inter-pore distance, wall thickness and barrier layer thickness. Pore diameter is directly related to anodizing potential [102].

D_P 1.20 $nmV^{-1}U$

D_P = pore diameter

U = anodizing potential

As shown by anodization in sulfuric acid, pore diameter depends on temperature for anodizing in sulfuric acid. An increased temperature causes increased pore diameter. The pore diameter can be widened in phosphoric acid. The pore diameter is also dependent on size, which is related to the steady state achieved during anodization when the current voltage curve becomes stationary. Another important factor is the inter-pore distance as it allows determining the number of pores per unit area. Figure 18 shows the inter-pore relationship to anodizing potential mechanism of oxide formation. The anions of the acid are transferred to the oxide/electrolyte interface. The acid anions can form OH^- or O_2^{-2}:

$$2Al + 6OH^- \rightarrow Al_2O_3 + 3H_2O + 6e^-$$

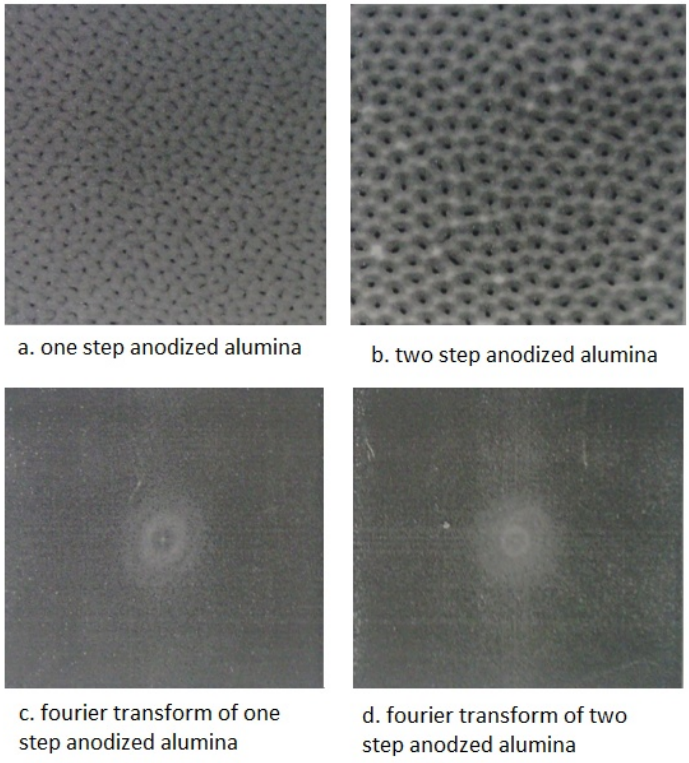

Figure 17. SEM images of one and two step anodization and their Fourier transforms.

$$2Al + 3O^{2-} \rightarrow Al_2O_3 + 6e^-$$

The oxides can also grow on oxide, electrolyte, and interface leading to the following reaction:

$$2Al + 6H_2O \rightarrow Al_2O_3 + 6H^+$$

The theory of formation of self-organized nano-pores is not well understood. It is popularly believed that there is a strong competition between the oxidation at the metal/oxide and dissolution of aluminum at the oxide/ electrolyte interface [102]. The process of anodization is followed by depositing a hydrophobic surface. The corrosion resistance of several aluminum alloys has been described in the earlier section; however, the effect of pore diameters, inter-pore spacing, shape of pores, hydrophobicity is not conclusively understood. The morphology of hydrophobic surfaces of aluminum alloys affects their corrosion resistance; however, the mechanism is not well understood.

http://dx.doi.org/10.5772/60815

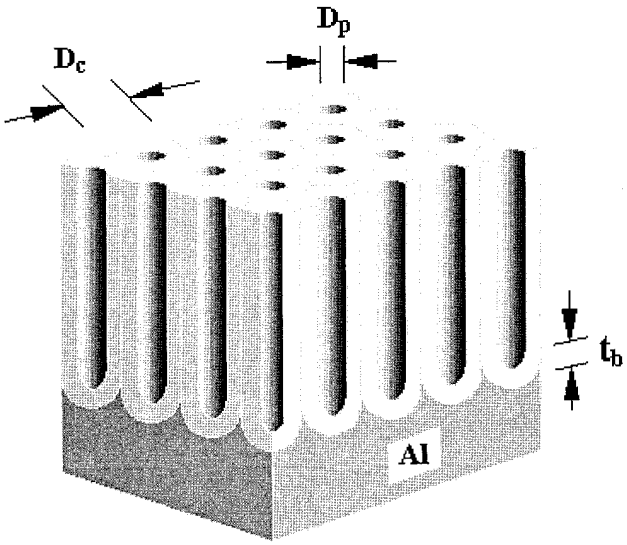

Figure 18. Ideal hexagonal "alumite" or PTF. Metallic Al, on the bottom, is covered by an impervious "barrier" oxide of thickness t_b and then by a hexagonal array of pores of diameter *D*p, with a cell (repeat) distance *D*c [101].

6.2. Effect of hydrophobic surface on corrosion resistance of copper alloys

It has been described earlier that the degree of corrosion of nano-structured materials is related to their micro-structure; in terms of crystallographic structure, porosity impurities, and triple junction [103], much depends on the homogeneity of the surface filmed formed. Whereas improved corrosion resistance has been reported for nano-crystalline $Al_{90}Fe_5Gd_5$ and $Al_{87}Ni_8Y_{43}$ and $Fe_{73}Si_{10}B_{25}C_{13}$ films [104], reduced corrosion resistance has been reported for $Cu_{90}Ni_{10}$ alloy [105]. In a study, nano-crystalline copper was deposited on titanium substrate by electro-deposition technique. The nano-crystalline copper electrode showed lesser localized corrosion than polycrystalline copper electrode in 3.5 wt% NaCl because of the formation of passive films consisting of CuCl and CuO_2 [106]. The uniform film formed on the nano-structured surface protects the nano-crystalline copper from corrosion.

Hydrophobicity has played a leading role in corrosion protection of copper and copper alloys in marine environment. The surface of copper was polished by SiC papers (400-1500 grade), degreased with acetone, washed with distilled water, dried, and etched in 7M HNO_3 for 30 s. To deposit a hydrophobic surface, the specimens were immersed in an ethanol solution of n-tetradecanoic acid 0.06 M at room temperature for 10 days. They were rinsed with de-ionized water and ethanol and dried in air. Samples of tough pitch copper were used (C1100). The surface of copper showed a flower like structure as shown in Fig. 19 [107].

Potentiodynamic polarization studies were conducted. Their distinct regions were observed with respect to the polarization curves, maximum corrosion current (I_{max}), minimum corrosion current (I_{min}), and limiting current (I_{limt}). The minimum corrosion current is attributed to the

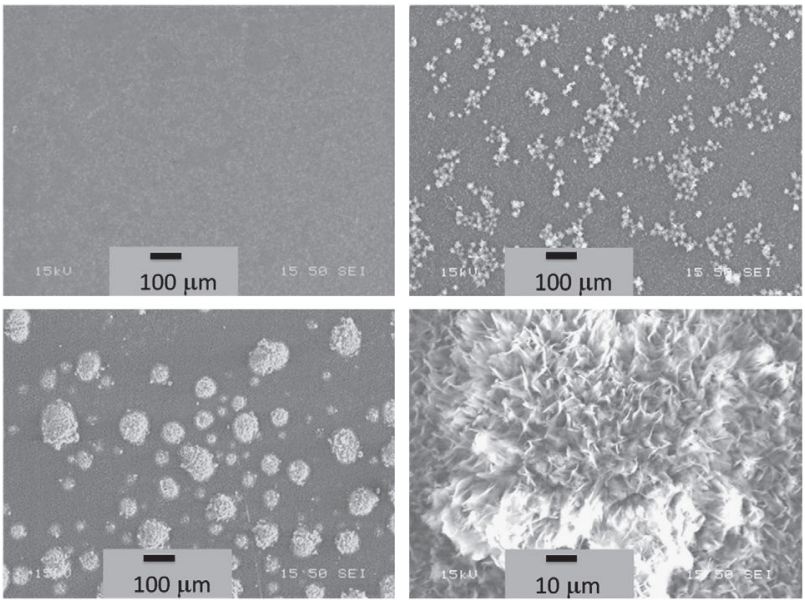

Figure 19. SEM images of the anodic surface of the copper electrode after the application of 30 V DC voltage in an ethanolic stearic acid solution for (a) 0.5 h, (b) 1.5 h, (c) 3 h, (d) the morphology of a single particle as observed after 3 h [107].

formation of CuCl layer. Dissolution occurs by formation of cuprous ions leading to enhance current.

$$Cu \rightarrow Cu^{+} + e^{-}$$

This is followed by the formation of CuCl, leading to minimization of corrosion current. The corrosion current again increases upon further increase of potential due to the formation of $CuCl_2$. The formation of CuCl and $CuCl_2$ can be represented by:

$$Cu + Cl^{-} \rightarrow CuCl$$

$$CuCl + Cl^{-} \rightarrow CuCl_2^{-}$$

The values of polarization resistance for the treated specimens A, B, D, and E were 6607, 8000, 6105, 5000, respectively, compared to the values of 2857, 500, 218, 6200 and 1233, 3000 respectively for F, C, and H (bare copper). Specimens A, B, D were chemically modified with myristic acid where as C, F, and H were untreated.

http://dx.doi.org/10.5772/60815

A composite state (Cassie Bexter regime) was formed by the flower like structure where water droplets were entrapped within the grooves, thus enhancing hydrophobicity [108]. Studies on suppression of copper have been conducted by anodizing copper in triazinedithiol (TDT) solution. Pre-treatment with TDT showed a very high corrosion resistance. It was indicated that the corrosion reaction is suppressed by increased number of carbon atoms in the hydrophobic radicals [109].

Self-assembled mono-layer technique has been used to protect copper, like on aluminum. Studies were made to compare the effects of SAMs of hexanethiol and hexaneselenol on copper surface. Vibrational sum frequency spectroscopy showed that the surface of hexaneselenol was removed during corrosion due to galvanic effect; this was in contrast to hexanethiol because of its stronger bond with the copper substrate. The mechanism is not, however, clearly understood [110].

A novel and facile method was developed to successfully fabricate a regular hierarchical surface structure on copper sheet via combination of polydimethylsiloxane (PDMS) template and chemical etching. After cleaning a fresh leaf of lotus, a liquid mixture of PDMS was mixed and cast on the cleaned lotus leaf and cured for 24 h. The PDMS was peeled off the lotus to obtain a porous PDMS template as shown in Fig. 20 [111].

To mimic the hydrophobic surface of the lotus flower, a 10 g $FeCl_3$ solution was prepared in ethanol. Simultaneously, a copper sheet and a glass slide were ultrasonically cleaned by HCl. The glass slide was firstly immersed horizontally in $FeCl_3$ for 20 min. It was withdrawn vertically from the solution slowly. This was followed by wetting of PDMS template with $FeCl_3$ and pressing gently against the glass slide. The copper plate was corroded with PDMS template and a pressure of 2.5 KN/m^2 was exerted for 24 h. The copper sheet was finally immersed in stearic acid to obtain a hydrophobic surface. A contact angle of 153^o was obtained. The surface mimicked the lotus leaf minimized corrosion. However, reliable data is not available and it offers a good scope for further work on the stability, adhesion, and corrosion resistance of a hydrophobic film [112].

Recently, attempts have been made to develop corrosion resistant hydrophobic grapheme oxide polymer composite coating on copper. The coating was deposited by electrophoretic technique. An aqueous dispersion of grapheme oxide was prepared (0.001-0.1g/L). A homogeneous solution of graphene and polymer was obtained by magnetic stirring and ultra-sonication for 20 min in an ultrasonic process. Electrophoretic deposition of polymer isocyanate associated with hydroxyl function acrylic adhesion was achieved as shown in Fig. 21 [113].

Two parallel plates of copper were used as electrodes, one acting as a cathode and the other acting as auxiliary electrode. Electrophoresis was performed at 10- 30 V. The deposition time ranged from 5 to 50 s. The deposit was treated with silicone to increase the hydrophobicity. Potentiodynamic polarization tests were conducted in 3.5 wt% NaCl to study the corrosion behavior of GOPC composite samples. The tafel plots of bare copper and GOPC coated copper are shown in Fig. 21. Images taken by FESEM shows that copper coated by composite and treated by silicone fluid shows no evidence of corrosion as shown by the uncoated copper

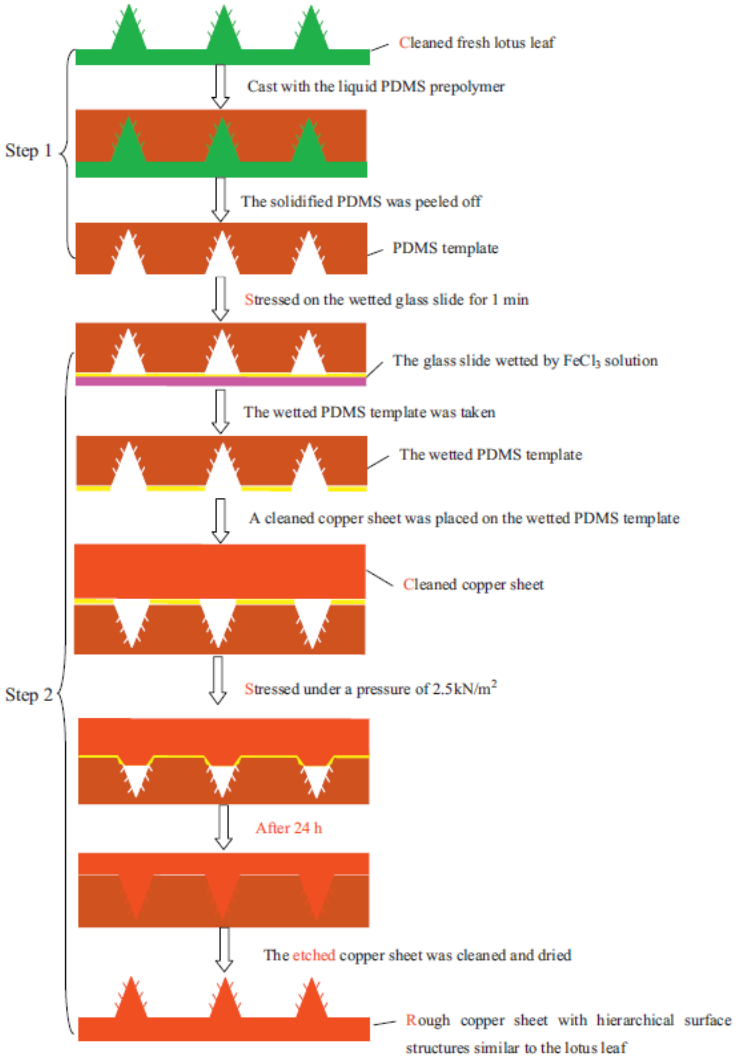

Figure 20. Procedure scheme for fabricating the lotus-leaf-like surface structures [111].

substrate. The corrosion resistance may be attributed to the formation of metal hydroxide at the electrode during electrophoresis deposition. The electrochemical impedance spectra showed the highest value for corrosion resistance for the sample coated with the GoPc [113] as shown in Fig. 22.

Enhancing the corrosion resistance of pure copper and copper alloys is extremely important because of a wide range of its application in marine, aggressive, and humid environments.

http://dx.doi.org/10.5772/60815

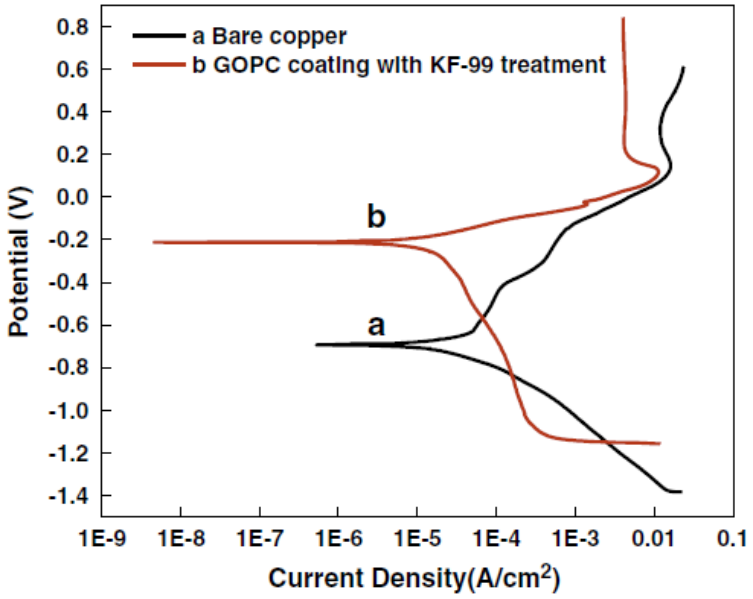

Figure 21. Tafel plots of (a) bare copper (b) GOPC coated copper after KF-99 treatment [113].

Cost-effective methods for industrial applications need to be developed to meet the increased industrial demand.

6.3. Effect of hydrophobic surface on the corrosion resistance of steels

Nano-structure plays a leading role not only in the creation of hydrophobic surfaces, but also on the corrosion resistance because of the grain size. TiO_2 thin films have been extensively used because of their applications in solar energy, photocatalytic reactors and anti-microbial properties [115-117]. Several methods have been used to fabricate thin TiO_2 films, e-beam evaporation, sputtering, chemical vapor deposition, physical vapor deposition, SAMs, and several other techniques [118-122]. The sol-gel technique has been the most popular because of its lesser equipment requirements and being a simple technique. In a work on preparation of hydrophobic surface on steel by sol-gel techniques, the optimum temperature for uniform distribution of nanoparticles was found to be 400°C. The average roughness was around 10.61 nm [123].

Chrome Moly steels are known to possess a useful combination of improved mechanical properties and high resistance to corrosion. These steels are widely employed in power generation plants. Samples of Cr-Mo steels were anodized to create roughness. The electrolyte was 1 M sulfuric acid and 0.16 M hydrofluoric acid and followed by pickling in hydrochloric acid. The samples were dipped for 10 days in myristic acid to obtain a hydrophobic surface. The AFM images showed a smooth and efficient coating. After exposing in myristic acid for

10 days, a wet contact angle of 148±4° was obtained. The contact angle depends on several factors such as surface roughness, size of crystallites (nano) and exposure period in solution used for making hydrophobic surfaces, such as fatty acids as in the above case. The electrochemical studies showed shifting of corrosion potential to more noble values, indicating the passivation of the surface. Electrochemical impedance studies showed an increase in charge transfer resistance (1.3×10^{11} Ω cm^2) and a lowering of capacitance values (2.0×10^{4} F/cm^2s^{-1}), which indicated the enhanced corrosion resistance of 9Cr-1Mo steel due to its hydrophobic surface. Not only the corrosion resistance but the tendency to attack micro-organisms in sea-water is significantly decreased. Several studies on bio-fouling have suggested that the attachment of microbial organism is reduced whereas some studies claim complete detachment of bio-films and microbial attachment [124].

A uniform TiO_2 film was created on the surface of a 316 stainless steel by sol-gel technique. The specimens were ground with 1 and 0.3 μm Al_2O_3 powder and ultra-sonically cleaned in distilled water. This was followed by heating to 450°C for 30 min. In order to avoid cracking, the samples were subjected to heating in boiling water for 10- 50 min followed by treatment in an oven at 450°C. The specimens were treated with fluoroalkyl-silane (FAS-13) to obtain a hydrophobic surface. The specimens were put in a dark room to avoid any photochemical effects. The polarization curves for 316 stainless steel in oxygen- saturated Ringer solution are shown in Fig. 22 [125].

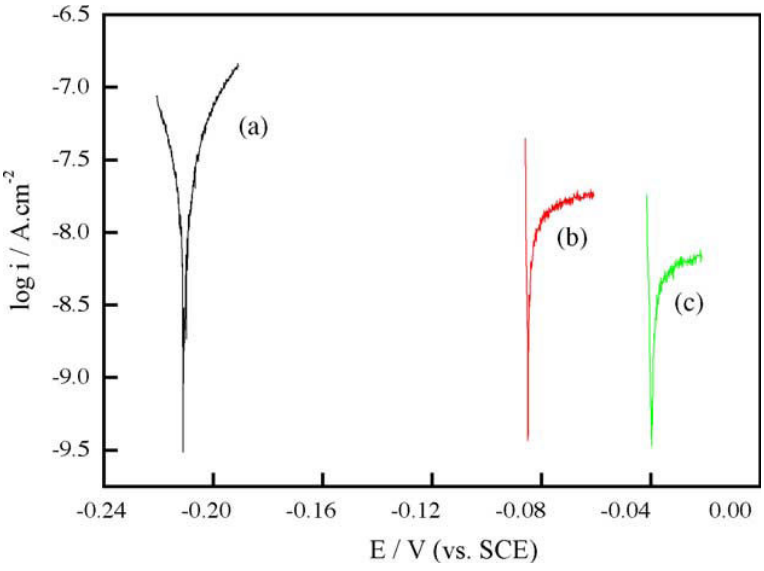

Figure 22. Polarization curves for bare 316L and films in oxygen-saturated Ringer solution. (a) Bare 316L; (b) TiO_2 / 316L coatings; (c) FSA/TiO_2 /316L coatings [125].

http://dx.doi.org/10.5772/60815

The nano-TiO_2 coated and FAS/nano- TiO_2 coated 316 stainless steel electrodes exhibited lower current densities. The corrosion potential (Ecorr) of FAS/nano- TiO_2 coated shifted to more noble values (-0.4V vs. SCE). This may be attributed to the formation of surface grooves, where gas is trapped and oxygen concentration is not disturbed and consequently the cathodic reaction is enhanced. The phenomenon is not clearly understood and more research is needed to find a conclusive mechanism. Work on impedance spectroscopy showed a low value of capacitance (10^{-8}) which reflects the insulating nature of the coating. The above work was pioneering for steels and it showed that the technique could be applied on a large scale for corrosion protection [114]. Super-hydrophobic surfaces on hastelloy with contact angle greater than 170° have been fabricated by sol-gel technique [126].

The hastelloy was pre-treated by ultra-sonic cleaning in acetone, alcohol and de-ionized water. The alloy was dip coated from TiO_2 pre-cursor containing TiO_2 nanoparticles (25 nm) followed by heat treatment. An aggregation of nanoparticles (150- 200 nm) was generated to create a hierarchical surface, a pre-requisite for the fabrication of a hydrophobic surface. The surface was treated with a 10 wt% ethanol solution of FAS-17, to generate hydrophobicity. The specimens were washed and dried at 140°C. The contact angle measured was 156.7°.

To evaluate the corrosion resistance, the alloy was exposed to hydrochloric acid, nitric acid, sulfuric acid, acetic acid, and sodium hydroxide. The bare hastelloys surface showed corrosion in the above media, as indicated by a color change of the substrate whereas no corrosion was observed on the hydrophobic surface. The wet contact angles and hysteresis showed that the magnitude of corrosion affects the degree of these angles. The higher contact angle before corrosion was 173°, which decreased with the degree of corrosivity. The high degree of wet contact angle and maintenance of hydrophobicity in highly corrosive environment suggests extended application of hastelloy in highly corrosive environment.

Hydrophobic surface on stainless steel may be obtained also simply by making the surface rough by etching, followed by electrolysis plating in a silane. A stainless steel plate was sandblasted with 200 μm silicon dioxide under a pressure of 0.4 mPa for 30 s and cleaned ultrasonically. This was followed by immersion in heptadecafluoro-1, 1, 2, 2, tetrahydrodecyl trimethoxy silane (HFTHTMS) to generate a super-hydrophobic surface prior to hydrophobic treatment, it was immersed in a plating bath of 1 mol/L $NiSO_4$ + $6H_2O$ + 0.25mol/L N_2H_4 for 4 h at 80°C at a pH value in the range 8- 10. Corrosion studies on the hydrophobic surface were conducted by potentiodynamic polarization. The steel (nickel coated) with a hydrophobic surface showed a more noble potential. Potentiodynamic polarization curves for the stainless steel in 3.5 wt% NaCl solution are shown in Fig. 23.

The porosity value (1.29) was very small, which significantly showed the compactness of the hydrophobic film. The possibility of micro-galvanic corrosion cannot be ignored in view of small valueΔEcorr. The effect of direct immersion in HFTHTMS with corrosion behavior of stainless steel after surface roughening is not known. A contact angle of 150° was maintained even after three months of exposure [125]. The relation between corrosivity and contact angle is not well understood and it needs a better understanding.

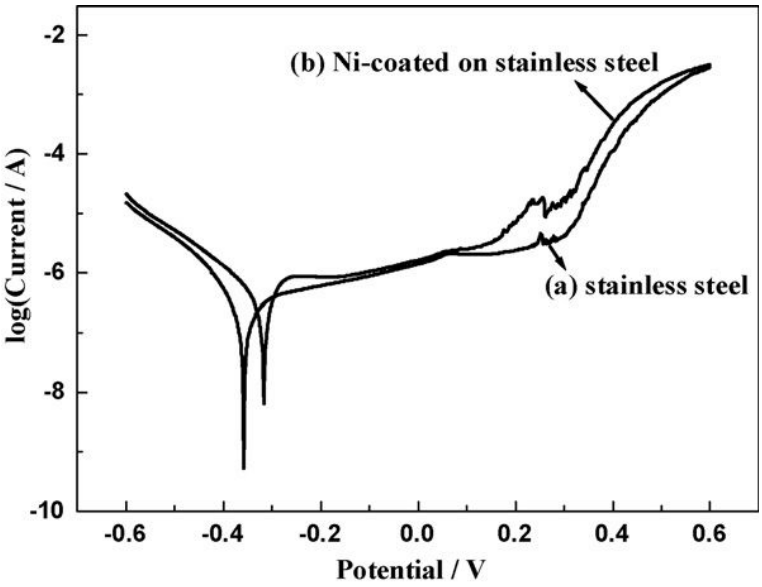

Figure 23. Potentiodynamic polarization curves for the stainless steel in 3.5 wt% NaCl solution (a) and the Ni-coated stainless steel (b) [125].

In a study, steel samples were coated with trimethoxypropyl silane (TMPS), polytetrafluoroethlylene (PTFE), and silica nanoparticles (NPS) to determine the effect of hydrophobicity on the corrosion resistance of carbon steels in salt solution [127]. Samples of steel, steel/silane, steel/silane/PTFE, steel/silane/NPS/PTFE were exposed to NaCl solution to determine their corrosion resistance. The results revealed that the samples coated with PTFE and NPS (nanoparticles) considerably improved the anti-corrosion resistance due to the formation of super-hydrophobic films on their substrate.

In a similar work, the corrosion inhibition of carbon steel in hydrochloric acid using sodium dodecylsulfonate was investigated [128]. The inhibitors used were dodecylsulfonate, $NaC_{12}H_{25}SO_3$ (SDSO), and ethyletherpolyoxyethylene. The tests were conducted in acidic solutions. The addition of SDSO in various concentrations of hydrochloric acid, increased concentration of SDSO, strengthened the inhibiting efficiency in various concentrations of hydrochloric acid because of adsorption of sulfonate through oxygen atom of sulfonate, by forming a barrier layer on the cathodic sites. At an SDSO concentration of 5.33×10^3 mol.dm^2, an abrupt decrease in efficiency was observed due to change from a hydrophobic to hydrophilic state. The effect of addition of $FeCl_3$, KCl, and $CaCl_2$ was also observed on the inhibition efficiency. It was observed that $FeCl_3$ addition increased the inhibition efficiency. It was attributed to an increase in Zeta Potential on the surface of carbon steel which leads to an increase in the adsorption density. It was observed that K^+ and Cl, Ca^{2+} ions had a weaker influence. A commercial surfactant Brij58 added to SDSO increased the inhibitor efficiency because of the adsorption of two surfactants.

http://dx.doi.org/10.5772/60815

Produced water in oil and gas industry is highly corrosive because of the presence of chlorides, dissolved CO_2, salinity and H_2S contents. Use of high performance alloys such as 316L, 2205, 20Cb-3, C-22 is effective, but they may increase the cost of the system by as much as five fold. Silicone based materials provide a cost effective alternative as they have the capability not only to reduce corrosion but also to minimize water surface interaction due to their hydrophobic nature. Tests were conducted on coupons coated with amorphous silicon or carbo-silane by chemical vapor deposition. On conducting immersion tests according to ASTM G31, in 6M HCl, the highest weight loss was shown by 316 stainless steel and the least (3.29) by carbo-silane-coated steel (91.90 vs. 3.29) equivalent to an overall mpy improvement of 27.9X over 316 stainless steel. The corrosion potential (Ecorr), corrosion current (Icorr), pitting potential of 316L, a-316L, and 304 were determined electrochemically. The data obtained suggested a 50x reduction in corrosion rate for Si-coated coupon in 3000 ppm Cl^- solution. The Si-coated coupon also showed no corrosion in salt spray tests in 3.5 wt% of NaCl. The reduction in corrosion of Si-coated 316 stainless steel was attributed to its inherent property of hydrophobicity, which was determined by wet contact angle.

The carbo-silane coating determined a higher degree of hydrophobicity with lesser hysteresis indicating a reduction in wetted area. Comparative studies on adsorption of water on commercial stainless steels showed that they adsorbed most water whereas electro-polished stainless steel tubes minimized adsorption. It was shown that a Si-coated electro-polished steel reduced corrosion further by 50%. The results show that hydrophobic surfaces minimize water adsorption on steel surface. It was further shown that a-Si coated electro-polished stainless steel specimen dried in 83% less time compared to the drying time of 180 min taken by an uncoated 316 stainless steel [129].

One of the recent areas of interest is the application of hydrophobic surfaces in prevention of corrosion of steel in concrete (re-bar corrosion). A serious problem is encountered by corrosion damage under de-icing salts. The molecular attraction between water and concrete is weakened by application of hydrophobic agents such as silanes and siloxanes. One important siloxane used is polydimethylsiloxane (PDMS). The structure of monomer of PDMS is shown in Fig. 24.

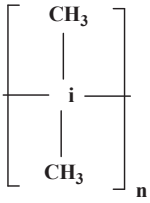

Figure 24. Structure of PDMS.

Silane particles are hydrophobic and they are functionalized by different silanes, for example fluoroalkyl-silanes, tri-chloroethylsilanes, perfluoroalkylsilanes, and several others.

The studies were carried out in concrete with W/C ratio of 0.50. Two types of concrete were used; portland cement and blast furnace slag cement, that is OPC and BFSC, respectively. Three commercially available hydrophobic products were used; a 99% silane (0 solvent), 100% silane (0 solvent), 20% silane/siloxane dispersed in water to determine the effect of hydrophobicity on the ingress of chloride after 52 weeks. It was observed that the chloride content was between 0.2% and 0.55 by mass of cement at a depth of 16- 20 mm in OPC and BFSC concrete, respectively, compared to 2.8% and 2.4% in untreated concrete, respectively, which was a significant reduction [130]. The question concerns the durability of the treated surface and it is feared that carbonation may occur after five years due to complete drying out of the surface. The water repellent surface minimizes carbonation of concrete.

7. Iceophobic surfaces

A new development of hydrophobic concretes has shown anti-icing properties (iceophobic). Iceophobic concrete reduces the ice adhesion on roadways and pavements. Super-hydrophobic admixtures, siloxanes, have been successfully developed. The admixtures are based on combination of siloxane- based hydrophobic liquid and small quantity of silica to form polymethyl-hydrogensiloxane. The super-hydrophobic surface reduces the ice bonding strength. The need for maintenance is hugely reduced with the use of iceo-phobic cementitious composites which, provide durability and strength [131].

Accumulation of ice is a serious problem in terms of life of equipment as it involves huge costs. It is a serious problem on aircraft, motor vehicles, power lines, decks, and bridge nuts. It is known that icing on aircraft can reduce their life by 30% and increase the drag by 10%. Heavy icing has led to air crashes in the past. De-icing of aircraft varies from country to country. In Netherlands, the cost of de-icing is 3000 Euros for Boeing 737. The cost of anti-icing treatment on private jets ranges from 250 Euros for a propeller jet to 10, 000 Euros. The price is based on the de-icing fluids required for removing ice. The cost of de-icing of motor vehicle ranges from 125 to 200 dollars depending on the size. Considering the number of vehicles affected by icing in the cold regions of the globe, the cost reaches highly alarming figures. Although the existing research on super-hydrophobic surfaces has not addressed the problem directly, it has offered hope for a future solution for de-icing. Research work has shown that the freezing time is substantially delayed on a super-hydrophobic surface [132]. Ice that accumulates on a super-hydrophobic surface in the Cassie Bexter state is weakly bonded and easy to remove. A new concept of Slippery Liquid Infused Porous Surface (SLIPS) [133] may be used to generate surfaces that are super-iceo-phobic. Attempts have been made to fabricate a network of Teflon nano-fiber and infuse in it a low surface energy perfluorinated fluid. Compounds such as 3 M fluorinate FC-80 and Du-pont Krytoxin (lubricating compound) have been used. SLIPS repelled water ~ 675 atm, which is hundred times the highest recorded pressure on super-hydrophobic surfaces. It showed very superior ice-repelling properties. The anti-icing properties of nanoparticle composites have been recently investigated [134]. Nanoparticles polymer composite has shown a high promise of iceophobicity. The anti-icing property depends not only on the nano-polymer composite but also on the particle size. Further

http://dx.doi.org/10.5772/60815

development would need a greater understanding of the hydrodynamic structure of the water film and the mechanism of adhesion of ice in relation to surface morphology.

8. Conclusion

The phenomena of hydrophobicity bestowed by nature on several biological objects, such as the lotus flower and the wings of butterflies, has evoked a great academic and industrial interest. Super-hydrophobicity is now recognized as one of the top fifty technologies. Research in the last decade has clearly shown that it is addressing serious problems such as those related to corrosion and bio-fouling, as shown by successful applications of hydrophobic surfaces in engineering systems such as aircraft, automobiles, pipelines, and naval vessels. By reducing the drag force and bio-fouling, these surfaces are playing a vital role in fuel saving. The fabrication of hydrophobic surfaces has undergone a significant transformation from highly complex processes to simple one step facile processes. Several techniques such as physical vapor deposition, chemical vapor deposition, magnetic sputtering, layer by layer, spin coating, spraying, self-assembled monolayer, and sol-gel techniques, however, are simple and they have evoked a great interest in recent years. The interest of researchers is mainly focused on aluminum, copper, and steel alloys. Increasing attention is being given to fabricate hydrophobic surfaces on glasses to impart self-cleaning and anti-fogging properties due to its important applications in land, sea, and air transport, but also its applications in optical lenses. Super-hydrophobic surfaces have shown enhanced corrosion resistance on Al alloy and are widely used. The effect of nano-pores, that is pore diameter, inter-pore diameter, plays an important role on the efficiency of hydrophobic coatings on aluminum alloys.

The corrosion resistance of copper based alloys has been significantly enhanced by coating with myristic and stearic acid. Hydrophobic surface on copper is likely to play a leading role in energy saving because of the jumping droplets phenomena observed on hydrophobic surface deposited on copper and copper wires. Surface morphology of hydrophobic surface plays a crucial part in its stability and wet contact angle. Surface roughness and deposition of low energy compounds are the key parameters for hydrophobicity. Surface roughness has been achieved in copper and aluminum alloys by anodizing at specific voltages for specific times. Etching has been used to create a rough surface on steel. Several other techniques have been used such as shot blasting, sand blasting, ultra-shot penning, and cavitation shot penning to obtain a nano-structured surface with grain size in the nano-range. Hydrophobic agents such as perfluorosilane, trimethoxypropyl silane, polydimethyl siloxane, 3-glycidoxypropyl-trimethoxy silane (GTPMS), trimethoxysilane (TEOS) have been extensively used to fabricate hydrophobic surfaces.

More recently, hydrophobicity has ushered a new era in clean building construction industry to address pollution and energy conservation. The emerging area which began from the observation of water and dust repelling properties of the lotus flower has now been successfully mimicked by scientists on engineered surfaces and it has successfully extended to all phases of engineering applications with dramatic effects on corrosion and bio-fouling.

Author details

Zaki Ahmad*, Asad U. Khan, Robina Farooq, Naila Riaz Mastoi and Tahir Saif

*Address all correspondence to: zakiahmad100@gmail.com

Department of Chemical Engineering, COMSATS Institute of Information Technology, Lahore, Pakistan

References

[1] R. S. Razavi, G. R. Gordani, "Laser surface treatments of aluminum alloys" in "*Recent Trends in Processing and Degradation of Aluminum Alloys"*, Ed. Zaki Ahmad, Intech open, Croatia, 2011, 115-154

[2] T.R. Davies (Ed), *Corrosion of Aluminum and Aluminum Alloy*, ASM International Materials Park, Ohio, USA, 1999, 44073-0002.

[3] K. Nisancioglu, H. Holter, Correlation of the open-circuit and electrochemical measurement for pitting corrosion of aluminum in chloride media, *Mater Corr*, 2004, Vol. 30(2), 115-113.

[4] Trung Hung Nguyen, R.T. Foley, On the mechanism of pitting of Aluminum, for electrochemical Soc *Electrochem Sci Technol*, 1979, Vol. 124 (11), 1855-1860.

[5] Saravanan Nagappa, Chang-Sik Ha, Emerging trends in superhydrophobic surface based magnetic materials: fabrications and their potential applications, *J Mater Chem A*, 2015, Vol. 3, 3224-3251.

[6] Ruomei Wu, Shuquan Liang, Jun Liu, Anqiang Pan, Y. Yu, Yan Tang, Fabrication of the micro/nano-structure superhydrophobic surface on aluminum alloy by sulfuric acid anodizing and polypropylene coating, *J Nanosci Nanotechnol*, 2013, Vol. 13, 2362–2368.

[7] Ying Huang, D.K. Sarkar, X-Grant Chen, Fabrication of superhydrophobic surfaces on aluminum alloy via electrodeposition of copper followed by electrochemical modification, *Nano-Micro Lett*, 2011, Vol. 3 (3), 160-165.

[8] Zhijin Gong, Jianli Wang, Limei Wu, Xiaoyu Wang, Guocheng Lu, Libing Liao, Fabrication of super hydrophobic surfaces on copper by solution-immersion, *Chin J Chem Eng*, 2013, Vol. 21 (8), 920–926.

[9] Xi Yao, Qinwen Chen, Liang Xu, Qikai Li, Yanlin Song, Xuefeng Gao, David Que´re, Lei Jiang, Bioinspired ribbed nanoneedles with robust superhydrophobicity, *Adv Funct Mater*, 2010, Vol. 20, 1–7.

[10] Jinming Xi, Lin Feng, Lei Jiang, A general approach for fabrication of superhydrophobic and super-amphiphobic surfaces, *Appl Phys Lett*, 2008, Vol. 92 (5), 053102-053103.

[11] Xia Zhang, Yonggang Guo, Yue Liu, Xue Yang, Jieqiong Pan, Pingyu Zhang, Facile fabrication of superhydrophobic surface with nanowire structures on nickel foil, *Appl Surf Sci*, 2013, Vol. 287, 299–303.

[12] Mei Li, Jianhai Xu, Qinghua Lu, Creating superhydrophobic surfaces with flowery structures on nickel substrates through a wet-chemical-process, *J Mater Chem*, 2007, Vol. 17, 4772-4776.

[13] Y.W. Hu, S. Liu, S.Y. Huang, W. Pan, Fabrication of superhydrophobic surfaces of titanium dioxide and nickel through electrochemical deposition on stainless steel substrate, *Key Eng Mater*, 2010, Vol. 434-435, 496-498.

[14] Zhongwei Wang, Qing Li, Zuxin She, Funan Chen, Longqin Li, Xiaoxu Zhang, Peng Zhang, Facile and fast fabrication of superhydrophobic surface on magnesium alloy, *Appl Surf Sci*, 2013, Vol. 271, 182–192.

[15] Jun Liang, Zhiguang Guo, Jian Fang, Jingcheng Hao, Fabrication of superhydrophobic surface on magnesium alloy, *Chem Lett*, 2007, Vol. 36 (3), 416-417.

[16] Qin Liu, Dexin Chen, and Zhixin Kang, One-step electrodeposition process to fabricate corrosion-resistant superhydrophobic surface on magnesium alloy, *ACS Appl Mater Interf*, 2015, Vol. 7 (3), 1859–1867.

[17] B.V. Mahesh, R.K. Singh Raman, Role of nanostructure in electrochemical corrosion and high temperature oxidation: a review, *Metall Mater Trans* A, 2014, Vol. 45A, 55799-55822.

[18] Rajeev K. Gupta, R.K. Singh Raman, Carl C. Koch, B.S. Murty, Effect of nanocrystalline structure on the corrosion of a Fe.20Cr alloy, *Int J Electrochem Sci*, 2013, Vol. 8 (5), 6791-6806.

[19] K.D. Ralston, N. Birbilis, Effect of grain size corrosion: a review, *Corrosion*, 2010, Vol. 66 (6), 0750051-07500513.

[20] X.Y. Wang, D.Y. Li, Mechanical and electrochemical behavior of nanocrystalline surface of 304 stainless steel, *Electrochem Aceta*, 2002, Vol. 47 (9), 3939-3947.

[21] T. Ishizaki, Y. Masuda, M. Sakamoto, Corrosion resistance and durability of superhydrophobic surface formed on magnesium alloy created with nanostructured cerium oxide film and fluoroalkylsilane molecules in corrosive NaCl aqueous solutions, ACS Publications, *Langmuir*, 2011, Vol. 27, 4780-4788.

[22] R.F. North, M.J. Pryor, The influence of corrosion product structure on the corrosion rate of Cu-Ni alloys, *Corr Sci*, 1970, Vol. 10 (5), 297-311.

[23] The nickel development institute, The Halloway, Alvechurch, Birmingham, B48, 7QB UK.

[24] K. Lu, Nanocrystalline metals crystallized from amorphous solids: nanocrystallization, structure and properties, *Mater Sci Eng*, R16, 1996, Figure 1, 162.

[25] Atul H. Chokshi, Triple junction limited grain growth in nanomaterials, *Script Mater* 2008, Vol. 59, Figure 1, 727.

[26] J. K. Yu, E. H. Han, L. Lu, X. J. Wei, Corrosion behaviors of nanocrystalline and conventional polycrystalline copper, *J Mater Sci*, 2005, Vol. 40, Figure 2, 1020.

[27] J.E. Switzer, G.J Shiflet, J.R. Scully, Localized corrosion of Al 90Fe 5Gd and Al 87Ni 8.7Y 4.3 alloys in the amorphous, nanocrystalline, and crystalline states: resistance to micrometer-scale pit formation, *Electrochem Aceta*, 2003, Vol. 48, 1223-1224.

[28] A. Barbucci, G. Farne, P. Matteazzi, R. Riccieri, G. Cerisola, Corrosion behavior of nanocrystalline Cu90Ni10 alloy in neutral solution containing chlorides, *Corr Sci*, 1999, Vol. 41, 463-475.

[29] F.J. Cornwell, G. Wildsmith, P.T. Gilbert, Pitting corrosion in copper tubes in cold water service, *Corr J*, 1973, Vol. 8 (5), 202-209.

[30] J.K. Yu, E.H. Han., L. Lu, X.J. Wei, Corrosion of nano-crystalline and conventional poly-crystalline copper, *J Mater Sci*, 2005, Vol. 40, 1019-1022.

[31] S. Virtanen, J. Brunner, J. Wioka, 28th ES meeting # 322, 1987.

[32] Zaki Ahmad, Abdul Aleem, Mohammad Abbas, Effect of scandium doping on the corrosion resistance and mechanical behavior of Al-3Mg alloy in neutral chloride solutions, *Mater Sci App*, 2011, Vol.2, 244-250

[33] Zaki Ahmad, The properties and applications of Scandium-reinforced aluminum, *J Min, Met Mater Soc*, 2003, Vol. 55 (2), 35-39.

[34] Gerhardus H. Koch, Michiel P.H. Brongers, Neil G. Thompson, *Cost of Corrosion and Prevention Strategies in United States*, C.C Technologies Laboratories, Inc., 2001, Dublin, Ohio, USA.

[35] Ahmad Z, Corrosion phenomena in coastal area of Arabian Gulf, *Brit Corr J*, 1996, Vol. 31 (2), 191-197.

[36] Maria Salta, Julian A. Wharton, Paul Stoodley, Simon P. Dennington, Liam R. Goodes et al., Designing biomimetic anti-fouling surfaces, *Philo Trans Royal Soc* A. 2010, Vol. 368, 4729-4754.

[37] R. Jafari, M. Farzaneh, A simple method to create super-hydrophobic aluminium surfaces, *Mater Sci For* 2012, Vol. 706-709, 2874-2879.

[38] Rolla G, Ellingsen, J.E, Herlofson B, Enhancement and inhibition of dental plaque formation – some old and new concepts, *Biofouling*, 1991, Vol. 3, 175-181.

[39] M. Quiryen, H.C. Van Der Mei, C.L. Bollen, G.I. Geertsema-Doornbusch, H.J. Busscher, D. Van Steenberghe, Clinical relevance of the influence of surface free energy and roughness on the supragingival and sub-gingival plaque formation in man, *Coll Surf* B 2, 1994, Vol. 3, 25-31.

[40] Jan Genzer, Kirill Efimenko, Recent developments in super-hydrophobic surfaces and their relevance to marine fouling; a review, *Biofouling: J Bio-adhes Biofilm Res*, 2006, Vol. 22 (5), 339-360.

[41] C.S. Gudipati, J.A. Finlay, J.A. Callow, Maureen E. Callow, K.L. Wooley, The antifouling and fouling release performance of hyper-branched fluoropolymers (HBFP) – polyethylene glycol (PEG) composites coatings evaluated by adsorption of bio-macromolecules and the green fouling alga (ulva), *Langmuir*, 2005, Vol. 21, 3044-3053.

[42] D.J. Gan, A. Mueller, K.L. Wooley, Amphiphilic and hydrophobic surface patterns generated from hyper-branched fluoropolymers/linear polymer networks: minimally-adhesive coatings via cross-linking of hyper-branched fluoropolymers, *J Polym Sci: A Polym Chem*, 2003, Vol. 41 (22), 3531-3540.

[43] Kenneth R. Trethewey, John Chamberlain, *Corrosion: For Students of Science and Engineering*, Longman Scientific and Technical, London. 1988.

[44] Mars J.G. Fontana, *Corrosion Engineering*, McGraw-Hill Book Company, 1985, ISBN-10: -0070214638.

[45] L.L. Shrier, *Corrosion* Vol. 1 & 2, Newnes-Butterworths, London, 1979.

[46] Zaki Ahmad, *Principles of Corrosion Engineering and Corrosion Control*, Butterworth-Heinemann, 2006, ISBN: 978-0-7506-5924-6.

[47] Anil Kumar Sinha, *Ferrous Physical Metallurgy*, Butterworth, Boston, 1989.

[48] Michael F. Ashby, *Material Selection in Mechanical Design*, 3rd edition, Butterworth-Heinemann, 2013.

[49] W. Barthlott, C. Neinhuis, The lotus-effect: nature's model for self cleaning surfaces. *Int Text Bull*, 2001, Vol. 1, 08-12.

[50] Robert J. Daniello, Nicholas E. Waterhouse, Jonathan P. Rothstein, Drag reduction in turbulent flows over super-hydrophobic surfaces, *Phys Flu*, 2009, Vol. 21 (8), 085103

[51] Xi Zhang, Feng Shi, Jia Niu, Yugui Jiang, Zhigiang Q. Wang, Super-hydrophobic surfaces: from structural to functional application, *J Mater Chem*, 2008, Vol. 18 (6), 621-633.

[52] Michael Nosonovsky, Bharat Bhushan, Super-hydrophobic surfaces and emerging applications: non-adhesion energy green engineering, *Curr Opin Coll Interf Sci*, Vol. 14 (4), 270-280.

[53] J.N. Israelachvili, *Intermolecular and Surface Forces*, 2nd edition, Academic Press, New York, 1991, 7665-7669.

[54] S. Shibuichi, T. Yamamoto, T. Onda, K. Tsujii, Super water and oil repellent surfaces resulting from fractal structure, *J Coll Interf Sci*, 1998, Vol. 208, 287-294.

[55] R.N. Wenzel, Resistance of solid surfaces to wetting by water, *Ind Eng Chem*, 1936, Vol. 28, 988-994.

[56] A.B.D. Cassie, S. Baxter, Wettability of porous surface, *Trans. Faraday Soc*, 1944, Vol. 40, 546-551.

[57] Liangliang Cao, *Superhydrophobic Surface: Design, Fabrication, and Applications*, PhD Thesis, Graduate Faculty of Swanson School of Engineering, University of Pittsburgh, 2010.

[58] K. Tsujii, T. Yamamoto, T. Onda, S. Shibuichi, Super oil repellent surface, *Angew Chem* (Int Ed Engl), 1997, Vol. 36 (9), 1011-1012.

[59] Lin Feng, Zhongyi Zhang, Zhenhong Mai, Yongmei Ma, Biqian Liu, Lei Jiang, Daoben Zhu, A super-hydrophobic and super-oleophilic coating mesh film for the separation of oil and water, *Angew Chem* (Int Ed), 2004, Vol. 43 (15), 2012-2014.

[60] Charged superhydrophobic condenser surface may make power plants more efficient, http://science-beta.slashdot.org/story/13/10/04/1836234/charged-superhydrophobic-condenser-surface-may-make-power-plants-more-efficient

[61] Koji Takahashi, Tatsuya Ikuta, Kunihito Nagayama, Yasuyuki Takaka, Tanemasa Asano, Simple fabrication of hydrophobic surface for high-temperature microsystems, 7th International Conference on Miniaturized Chemical and Biochemical Analysts System, 2003, Squaw Valley, California, U.S.A.

[62] J.T. Han, Y. Zheng, J. H. Cho, X. Xu, K. Cho, Stable superhydrophobic organic-inorganic hybrid films by electrostatic self-assembly, *J Phys Chem* B 2005, Vol. 109 (44), 20773–20778.

[63] Lianbin Zhang, Huan Chen, Jungi Sun, Jiacong Shen, Layer-by-layer deposition of poly (diallyldimethylammonium chloride and sodium silicate multi-layers on silica sphere coated substrate – facile method to prepare a super-hydrophobic surface, *Chem Mater*, 2007, Vol. 19, 948-953.

[64] X. Zhang, F. Shi, X. Yu, H. Liu, Y. Fu, Z. Wang, L. Jiang, X. Li, Polyelectrolyte multilayer as matrix for electrochemical deposition of gold clusters: towards super-hydrophobic surfaces, *J Am Chem Soc*, 2006, Vol. 126 (10), 3064-3065.

[65] F. Shi, Z. Wang, X. Zhang, Combining a layer-by-layer assembling technique with electrochemical deposition of gold aggregates to mimic the legs of water striders, *Adv Mater*, 2008, Vol. 17 (8), 1005-1009.

[66] N. Zhao, F. Shi, Z. Wang, X. Zhang, Combining layer-by-layer assembly with electrodeposition of silver aggregates for fabricating super-hydrophobic surfaces, *Langmuir*, 2005, Vol. 21 (10), 4713-4716.

[67] F. Shi, J. Niu, J. Liu, Z. Wang, X.Q. Feng, X. Zhang, Towards understanding why a superhydrophobic coating is needed by water striders, *Adv Mater*, 2007, Vol. 19 (17), 2257-2261.

[68] S. Wang, L. Feng, H. Liu, T. Sun, X. Zhang, L. Jiang, D. Zhu, Manipulation of surface wettability between super-hydrophobicity and super-hydrophilicity on copper films, *Chem Phys Chem*, 2005, Vol. 6 (8), 1475-1478.

[69] J.P. Youngblood, T.J. McCarthy, Ultra-hydrophobic polymer surfaces prepared by simultaneous ablation of polypropylene and sputtering of poly(tetrafluoroethylene) using radio frequency plasma, *Macro-molecules*, 1999, Vol. 32 (20), 6600-6806.

[70] I. Woodward, W.C.E. Schofield, V. Roucoules, J.P Badyal, Super-hydrophobic surfaces produced by plasma fluorination of polybutadiene films, *Langmuir*, 2003, Vol. 19 (8), 3432-3438.

[71] Kenneth K.S. Lau, J. Bico, Kenneth B.K. Teo, Manish Chhowalla, Gehan A.J. Amaratunga, W.I. Milne, G.H. Mckinley, Karen. K. Gleason, Super-hydrophobic carbon nano-tube forests, *Nano Lett*, 2003, Vol. 3 (12), 1701-1705.

[72] Y. Wu, H. Sugimura, Y. Inoue, O. Takai, Thin films with nanotextures for transparent and ultra water-reppelent coatings produced from trimethylmethoxysilane by microwave plasma CVD, *Chem Vap Depos*, 2002, Vol. 8 (2), 47-50.

[73] Y. Wu, M. Bekke, Y. Inoue, H. Sugimura, H. Kitaguchi, C. Liu, O. Takai, Mechanical durability of ultra-water-repellent thin film by microwave plasma-enhanced CVD, *Thin Solid Films*, 2004, Vol. 457, 122-127.

[74] J.M. Lim, G.R. Yi, J.H. Moon, C.J. Heo, S.M. Yang, Super-hydrophobic films of electrospun fibers with multiple-scale surface morphology, *Langmuir*, 2007, Vol. 23, 7981-7989.

[75] A. Greiner, and J.H. Wendorff, Electrospinning: A fascinating method for the preparation of ultrathin fibres, *Angew Chem* (Int. Ed.), 2007, Vol. 46(30), 5670-5703.

[76] J. Bravo, L. Zhai, Z. Wu, R.E. Cohen, M.F. Rubner, Transparent super-hydrophobic films based on silica nanoparticles, *Langmuir*, 2007, Vol. 23 (13), 7293-7298.

[77] Y. Xiu, F. Xiao, D.W. Hess, C.P. Wong, Super-hydrophobic optically transparent silica films formed with a eutectic liquid, *Thin Solid Films*, 2009, Vol. 517 (5), 1610-1615.

[78] G.R.J Artus, S. Jung, J. Zimmermann, H.P. Gautschi, K. Marquardt, S. Seeger, Silicon nano-filaments and their applications as super-hydrophobic coatings, *Adv Mater*, 2006, Vol. 18 (20), 2758-2762.

[79] Kamal K. Gupta, Manjeet Jassal, Ashwini K. Agarwal, Sol-gel derived titanium dioxide finishing of cotton fabric for self cleaning, *Ind J Fiber Text Res*, 2008, Vol. 33 (4), 443-450.

[80] Violeta Purcar, Dan Donescu, Ilie Catalin Spataru et al., Surface modification of sol-gel hybrid films using fluorinated silica nanoparticles, *Revue Roumanie de Chimie*, 2013, Vol. 58 (1), 37-42.

[81] R.J. Nuzzo, D.L. Allara, Adsorption of bifunctional disulfides on gold surfaces, *J Am Chem Soc*, 1983, Vol. 105 (3), 4481-4483.

[82] Deepak Prashar, Self-assembled monolayers: a review, *Int J ChemTech Res*, Vol. 4 (1), 258-265.

[83] J.C. Love, L.A. Estroff, J.K. Kriebel, R.J. Nuzzo, G.M. Whitesides, Self-assembled monolayers of thiolates on metals as a form of nanotechnology, *Chem Rev*, 2005, Vol. 105 (4), 1103-1170.

[84] F. Shi, X. Chen, L. Wang, J. Niu, J. Yu, Z. Wang, X. Zhang, Roselike microstructures formed by direct in situ hydrothermal synthesis: from superhydrophophilicity to superhydrophobicity, *Chem Mater*, 2005, Vol. 17 (24), 6177-6180.

[85] Jakub Sirc, Radka Hobzova, Nina Kostina, et al., Morphological characterization of nanofibers: methods and application in practice, *J Nanomater*, 2012, Vol. 2012.

[86] D. Oner, T.J. McCarthy, Ultrahydrophobic surface, effects of topography length scales on wettability, *Langmuir*, 2000, Vol. 16 (20), 7777-7782.

[87] J.Y. Shiu, C.W. Kuo, P. Chen, C.Y. Mou, Fabrication of tunable superhydrophobic surfaces by nano-sphere lithography, *Chem Mater*, 2004, Vol. 16 (4), 561-564.

[88] Lester Li, Victor Breedveld, Dennis W. Hess, Creation of super-hydrophobic stainless steel surfaces by acid treatment and hydrophobic film deposition, ACS, *Appl Mater Interf*, 2012, Vol. 4 (9), 4549-4556.

[89] Boisier, Grégory and Lamure, Alain and Pébère, Nadine and Portail, Nicolas and Villatte, Martine, Corrosion protection of AA2024 sealedanodic layers using the hydrophobic properties of carboxylic acids. *Surf Coat Technol*, 2009, Vol. 203 (22), 3420-3426.

[90] Liu et al., New application potential of the underground super-hydrophobic surface in the corrosion protection, *Adv Mater Res*, 2009, Vol. 79 (82), 1115-1118.

[91] Liu et al., Inhibition microbial adherence of super-hydrophobic surface on aluminium in sea water, *Adv Mater Res*, 2009, Vol. 79 (82), 1123-1126.

[92] Samer Darwich, *Corrosion Protection Concepts for Aluminium and Magnesium Alloy Coated with Silica Films Prepared by Water Based Sol-Gel Process*, PhD Thesis, 2012, Technischen Universitat Chemnitz, Germany.

[93] Tian He, Yuanchao Wang, Yijian Zhang, Quan L.V, Tugen Xu, Tao Liu, Super-hydrophobic surfaces treatment as corrosion protection for aluminium in sea-water, *Corr Sci*, 2009, Vol. 51, 1751-1763.

[94] J. Bico, U. Thiele, D. Quere, Wetting of textured surfaces, *Coll Surf* A: *Physiochem Eng Asp*, 2002, Vol. 206, 41-46.

[95] R.I. Joned, A.D. Warren, D.M. Rosenberg, V.J. Bellito, R. Park, M.R. Zachariah, Surface passivation of bare aluminium nanoparticles using perfluoroalkyl carboxylic acids, *Chem Mater*, 2008, Vol. 17 (11), 2087-2996.

[96] Rodrigo S. Neves, Daiane P. B. Silva, and Artur J. Motheo, Corrosion protection of AA7075 aluminium alloy by trimethoxy-silanes self-assembled monolayers, ISRN *Electrochemistry*, 2013, Vol. 2013, Article ID 142493.

[97] Paul E. Hintze, Luz Marina Celle, Electrochemical properties and corrosion properties of organo-silane self-assembled mono-layer on aluminium 2024-T3, *Electrochem Aceta*, 2009, Vol. 51, 1761-1766.

[98] V. Palanivel, Y. Huang, W.J. Van Ooij, Effect of addition of corrosion inhibitors to silane films on the performance of AA2024-T3 in 0.5M NaCl solution, *Prog Org Coat*, 2005, Vol. 53 (2), 153-168.

[99] A. Ulman, Formation and structure of self-assembled monolayers, *Chem Rev*, 1996, Vol. 96 (4), 1533-1554.

[100] Feiyue Li, Lan Zhang, Robert M. Metzger, On the growth of highly ordered pores in anodized aluminum oxide, *Chem Mater*, 1998, Vol. 10, Figure 1, 2471.

[101] J.P. O'Sullivan, G.C. Wood, Morphology and mechanism of formation of porous anodic films on aluminium, *Proc Royal Soc London*, Series A, 1970, Vol. 317 (1731), 511-543.

[102] G. Plumbo, S.J. Thorpe, K.T. Aust, On the contribution of triple junctions to the structure and properties of nanocrystalline materials, *Scrip Metall Mater* 1990, Vol. 24, 1347-1350.

[103] R. Rofagha, R.Langer, A.M. El-Sheikh, U. Erb, G. Palumbo. K.T. Aust, The corrosion behavior of nanocrystalline nickel, *Scrip Metall Mater*, 1991, Vol. 25 (12), 2867-2872.

[104] S.J. Thorpe, B. Ramaswami, K.T. Aust, Corrosion and auger studies of a nickel based metal-metalloid glass I. The effect of elemental interactions on passivity in the general corrosion of metglass 2826A, *J Electrochem Soc*, 1988, Vol. 135 (9), 2162-2170.

[105] J.K. Yu, E.H. Han, L. Lu, X.J. Wei, M. Leung, Corrosion behavior of nano-crystalline and conventional polycrystalline copper, *J Mater Sci*, 2005, Vol. 49 (4), 1019-1022.

[106] Y. Huang, D.K. Sarkar, X. Grant Chen, A one-step process to engineer superhydrophobic copper surfaces, *Mater Lett*, 2010, Vol. 64, Figure 1, 2723.

[107] Felios Athanasios, *Corrosion Behavior of Super-Hydrophobic Film on Copper in Sea Water*, PhD thesis, 2012, National Technical University of Athens, School of Naval Architecture and Marine Engineering.

[108] H. Baba, T.K. Odana, K. Mon, The corrosion inhibition of copper by potentiostatic anodization in triazinedithiol solutions, *Corr Sci*, Vol. 39 (3), 556-564.

[109] Saman Hosseinpour, Mats Gothelid, Christofer Leygraf, C. Magnus Johnson, Self-assembled mono-layers as inhibitors for the atmospheric corrosion of copper induced by formic acid; a comparison between hexanethiol and hexaneselenol, *J Electrochem Soc*, 2014, Vol. 161 (C50-C56).

[110] Zhiqing Yuan, Xian Wang, Jiping Bin, Chaoyi Peng, Suli Xing, Menglei Wang, Jiayu Xiao, Jingcheng Zeng, Yong Xie, Ximei Xiao, Xin Fu, Huifang Gong, Dejian Zhao, A novel fabrication of a superhydrophobic surface with highly similar hierarchical structure of the lotus leaf on a copper sheet, *Appl Surf Sci*, 2013, Vol. 285(B), 205-210

[111] Z. J. Wei, W. L. Liu, D. Tian, C. L. Xiao and X. Q. Wang, Preparation of Lotus-Like Superhydrophobic Fluoropo- lymer Films, *Appl Surf Sci,* 2010, Vol. 256, 3972-3976.

[112] Bimal P. Singh, Bikash Kumar Jena, Sarama Bhattacharjee, Laxmidhar Besra, Development of oxidation and corrosion resistance hydrophobic grapheme oxide-polymer composite coating on copper, *Surf Coat Technol*, 2013, Vol. 232, 475-481.

[113] G.X. Shen, Y.C. Chen, L. Lin, C.J. Lin, D. Scantlebury, Study on the hydrophobic nano-TiO_2 coating and its properties for corrosion protection of metals, *Electrochem Aceta*, 2005, Vol. 50, 5083-5089.

[114] E.O. Zayim, Effect of calcination and pH value on the structural and optical properties of titanium oxide thin film, *J Mater Sci*, 2005, Vol. 40 (6), 1345-1352.

[115] B. O'Regan, M. Gratzel, A low cost, high efficiency solar cell based on dye-synthesized colloidal TiO_2 films, *Nature*, 1991, Vol. 353.

[116] M. Joshi, A. Bhattacharya, N. Agarwal, S. Parman, Nanostructured coatings for super-hydrophobic textiles, *Bull Mater Sci*, 2012, Vol. 35 (6), 933-938.

[117] S. Takeda, S. Suzuki, H. Odaka, H. Hosono, Photocatalytic TiO_2 thin film deposited onto glass by DC magnetron sputtering, *Thin Solid Films*, 2001, Vol. 392 (2), 338-344.

[118] H.Y. Ha, S.W. Nam, T.H. Lim, In. H. Oh, S.A. Hong, Properties of the TiO_2 membranes prepared by CVD of titanium tetraisopropoxide, *J Memb Sci*, 1996, Vol. 111 (1), 81-92.

[119] L. Hu, T. Yoko, H. Kozuka, S. Sakka, Effect of solvent on properties of sol-gel derived TiO_2 coating film, *Thin Solid Films*, 1992, Vol. 219 (1-2), 18-23.

[120] C.J. Brinker, G.W. Scherer, *Sol-Gel Science: The Physics and Chemistry of Sol-Gel Processing*, Academic Press, Inc, New York, 1990, 163-169.

[121] Z. Zainal, C.Y. Lee, Properties and photoelectrocatalytic behavior of sol-gel derived TiO_2 thin films, *J Sol-Gel Sci Technol*, 2006, Vol. 37 (1), 19-25.

[122] N. Barati, M.A. Faghihi Sani, H. Ghasemi, Z. Sadeghian, S.M.M. Mirhoseini, Preparation of uniform TiO_2 nano-structure film on 316 stainless steel by sol-gel dip coating, *Appl Surf Sci*, 2009, Vol. 255, 8328-8333.

[123] P.V. Mahalakshmi, S.C. Vanithakumari, Judy Gopal, U. Kamachi Mudali, R. Baldeve, Enhancing corrosion and biofouling resistance through super-hydrophobic surface modification, *Curr Sci*, 2011, Vol. 101 (10), 1328.

[124] Li Juan Chen, Miao Chen, Hui Di Zhou, Jian Min Chen, Preparation of super-hydrophobic surface on stainless steel, *Appl Surf Sci*, 2008, Vol. 255, 3459-3462.

[125] Hu Yawei, Huang Siya, Liu Shan, Pan Wei, A corrosion resistance super-hydrophobic TiO_2 film, *Appl Surf Sci*, 2012, Vol. 258 (19), 7460-7464.

[126] J.A. Nasdi, D.E. Weibel, A.F. Michels, F. Horowitz, Super-hydrophobic and anti-corrosion properties of silane/silica nanoparticles/PTFE coatings on carbon steel. Instituto de Quimica and Pgcimat Universidad Fereraldo Rio Grande do sul, Porto Alegre, RS, Brazil, 2012.

[127] Shazly Salem, Corrosion inhibition of carbon steel in HCl using sodium dodecyl sulfonate: the synergistic effect of non-ionic co-surfactant and some inorganic ions, *J Eng Sci*, 2011, Vol. 39 (5), 1147-1156.

[128] M. Higgins, D. Smith, J. Mattzela, G. Barone, Protective chemical vapor deposition coatings for stainless steel surfaces used in produced water environments, Silico Tek. Corporation, 112, Benner Circle. Bellefonte, PA, 16823, http://www.silcotek.com/

[129] Rob. B. Polder, Huibert Boreje, Prevention of re-inforcement corrosion by hydrophobic treatment of concrete, HERON, 2001, Vol. 46 (4).

[130] Anti-icing and de-icing super-hydrophobic concrete to improve the safety on critical element of roadway pavements and bridges, Sept. 2013, National center for freight and infrastructure research and education University of Wisconsin, Milwaukee, USA.

[131] P. Tourkine et al., Delayed Freezing on water repellent materials, *Langmuir*, 2009, Vol. 25 (13), 7214-7216.

[132] T.S. Wong et al., Bio-inspired self-repairing slippery surface with pressure stable omniphobicity, Nature, 2011, Vol. 477, 443-447.

[133] Liangliang Cao, Andrew K. Jones, Xinod K. Sikka, Jianzhong Wu, D. Gao, Anti-icing super-hydrophobic coating, Langmuir, 2009, Vol. 21, 1244-1248.